

# Performance Evaluation of Wimedia UWB MAC Protocols

by

Rukhsana Afroz Ruby

B.Sc., Bangladesh University of Engineering & Technology, 2004

A Dissertation Submitted in Partial Fulfillment of the  
Requirements for the Degree of

MASTER OF SCIENCE

in the Department of Computer Science

© Rukhsana Afroz Ruby, 2009

University of Victoria

All rights reserved. This dissertation may not be reproduced in whole or in part, by  
photocopying  
or other means, without the permission of the author.

# Performance Evaluation of Wimedia UWB MAC Protocols

by

Rukhsana Afroz Ruby

B.Sc., Bangladesh University of Engineering & Technology, 2004

Supervisory Committee

Dr. Jianping Pan, Supervisor  
(Department of Computer Science)

Dr. Sudhakar Ganti, Departmental Member  
(Department of Computer Science)

Dr. Kui Wu, Departmental Member  
(Department of Computer Science)

## **Supervisory Committee**

Dr. Jianping Pan, Supervisor  
(Department of Computer Science)

Dr. Sudhakar Ganti, Departmental Member  
(Department of Computer Science)

Dr. Kui Wu, Departmental Member  
(Department of Computer Science)

## **ABSTRACT**

Broadband Internet access technologies and Internet Protocol Television (IPTV) have enabled service providers to deliver high-definition video streams to the doorsteps of IPTV subscribers. On the other hand, how to distribute the high data rate, delay sensitive video traffic to almost all rooms in a typical household environment becomes a new challenge. There are several approaches proposed for IPTV in-home distribution, among which the wireless ones are very attractive due to their flexibility and affordability, but the physical and media access control (MAC) layer limitations in most existing wireless technologies still impend the success of video streaming over wireless networks. Recently, WiMedia Alliance has finalized its MB-OFDM based Ultra Wide Band (UWB) standards for Wireless Personal Area Networks (WPAN). WiMedia UWB supports two MAC protocols: Distributed Reservation Protocol (DRP) and Prioritized Channel Access (PCA), which are very suitable for high-quality video streaming. Based on our experimentation experience, the focus of our work is to

develop an analytical model for WiMedia UWB MAC protocols using the renewal reward theorem framework and quantify the video streaming performance considering all practical features (PCA, Hard DRP, Soft DRP, TXOP) of WiMedia MAC protocols. We have done extensive simulation in *NS-2* to validate the model and further evaluate the performance of WiMedia UWB MAC protocols.

# Contents

Supervisory Committee	ii
Abstract	iii
Table of Contents	v
List of Tables	viii
List of Figures	ix
Acknowledgements	xi
Dedication	xii
<b>1 Introduction</b>	<b>1</b>
<b>2 Background</b>	<b>6</b>
2.1 IEEE 802.11 WLAN . . . . .	7
2.2 IEEE 802.15 WPAN . . . . .	8
2.3 Ultra-Wide Band Technologies . . . . .	9
2.4 Overview of IEEE 802.11e . . . . .	10
2.5 Video Streaming over Wireless Networks . . . . .	12
<b>3 Related Work</b>	<b>13</b>

<b>4</b>	<b>Experimentation</b>	<b>17</b>
4.1	Evaluation Methodology . . . . .	18
4.1.1	Testbed Configuration . . . . .	18
4.1.2	Network Characterization . . . . .	20
4.1.3	Video Evaluation . . . . .	20
4.2	Performance Analysis . . . . .	22
4.3	Performance Results . . . . .	24
4.3.1	TxRate and Retry Limit . . . . .	24
4.3.2	Reservation Percentage and Pattern . . . . .	29
4.4	Summary . . . . .	34
<b>5</b>	<b>Analytical Models</b>	<b>36</b>
5.1	Saturated PCA without DRP . . . . .	39
5.2	Saturated PCA with DRP . . . . .	44
5.3	Unsaturated PCA without DRP . . . . .	44
<b>6</b>	<b>Video Streaming over UWB Wireless Networks Simulation</b>	<b>47</b>
6.1	Model Validation . . . . .	48
6.1.1	Simulation Methodology . . . . .	48
6.1.2	Validation of PCA Performance without DRP . . . . .	48
6.1.3	Validation of PCA Performance with DRP . . . . .	53
6.1.4	PCA performance and TXOP . . . . .	55
6.2	Performance Evaluation of Video Streaming over UWB Wireless Networks . . . . .	57
6.2.1	Soft and Hard DRP Implementation . . . . .	57
6.2.2	Methodology . . . . .	58
6.2.3	Collision Probability & Frame Service Time . . . . .	59

6.2.4	Packet Loss . . . . .	64
6.2.5	PSNR . . . . .	65
6.2.6	Frame Jitter . . . . .	67
6.2.7	Admission Region . . . . .	71
6.3	Summary . . . . .	71
<b>7</b>	<b>Conclusions and Future Work</b>	<b>75</b>
	<b>Bibliography</b>	<b>78</b>

# List of Tables

Table 4.1	Maximum Goodput (Retry Limit=0) . . . . .	27
Table 4.2	Reservation Patterns . . . . .	27
Table 4.3	Maximum Throughput (TxRate=53 Mbps) . . . . .	31
Table 5.1	Symbols Used in Model . . . . .	41
Table 6.1	Parameters Used for Performance Evaluation . . . . .	49



# List of Figures

Figure 4.1	Testbed Configuration. . . . .	18
Figure 4.2	Frame Size vs Frame Sequence Number. . . . .	21
Figure 4.3	Packet Loss vs TxRate and Retry Limit. . . . .	25
Figure 4.4	Goodput vs TxRate and Retry Limit. . . . .	26
Figure 4.5	Average PSNR vs TxRate and Retry Limit. . . . .	28
Figure 4.6	Throughput vs Reservation Pattern. . . . .	30
Figure 4.7	Packet Delay vs Packet Sequence Number. . . . .	32
Figure 4.8	Frame Jitter vs Reservation Pattern. . . . .	33
Figure 5.1	Renewal Reward Theorem . . . . .	37
Figure 5.2	Prioritized Contention Access With The Presence of DRP. . .	39
Figure 6.1	Network Topology . . . . .	49
Figure 6.2	Average Per Station Frame Service Time vs. Frame Arrival Rate	51
Figure 6.3	Average Per Station Frame Service Time vs. Frame Arrival Rate	51
Figure 6.4	Average Per Station Frame Service Time vs. The Number of Stations . . . . .	52
Figure 6.5	Average Per Station Frame Service Time vs. The Number of Stations . . . . .	52
Figure 6.6	Average Per AC1 Station Frame Service Time vs. Frame Ar- rival Rate . . . . .	53

Figure 6.7	Average Per AC2 Station Frame Service Time vs. Frame Arrival Rate . . . . .	54
Figure 6.8	Average Per Station Frame Service Time vs. Frame Arrival Rate	56
Figure 6.9	Collision Probability vs. The Number of DRP slots per station	61
Figure 6.10	Collision Probability vs. The Number of Video Streams . . . . .	62
Figure 6.11	Average Per Station Frame Service Time vs. The Number of DRP slots per station . . . . .	62
Figure 6.12	Average Per Station Frame Service Time vs. The Number of Video Streams . . . . .	63
Figure 6.13	I-Frame PLR (%) vs. The Number of DRP slots per station .	65
Figure 6.14	I-Frame PLR (%) vs. The Number of Video Streams . . . . .	66
Figure 6.15	Average PSNR (dB) vs. The Number of DRP slots per station	68
Figure 6.16	Average PSNR (dB) vs. The Number of Video Streams . . . . .	68
Figure 6.17	Maximum Accumulated Jitter (ms) vs. The Number of DRP slots per station . . . . .	70
Figure 6.18	Maximum Accumulated Jitter (ms) vs. The Number of Video Streams . . . . .	70
Figure 6.19	Admission Region With Soft DRP . . . . .	72
Figure 6.20	Admission Region With Hard DRP . . . . .	72

## ACKNOWLEDGEMENTS

First of all, I am very grateful to my supervisor Dr. Jianping Pan for his endless support, guidance and strong encouragement throughout my graduate study. In fact, he taught me how to do good research. Besides, I got lots of advice from him on how to become a successful researcher in the future.

I also would like to thank my thesis committee members: Dr. Sudhakar Ganti and Dr. Kui Wu for their valuable suggestions and help from time to time.

Finally I would like to thank my mother and sister for supporting me personally, so I can proceed so far.

DEDICATION

*To My Parents*

# Chapter 1

## Introduction

With the advent of whole-house entertainment applications such as Internet Protocol Television (IPTV) and Digital Video Recorder (DVR), the need for video distribution among almost all rooms in a household environment is obvious. Nowadays, service providers have the capability of delivering tens to hundreds of megabit-per-second (Mbps) to the doorstep of subscribers, but how to distribute the video, voice and data traffic within the premise of ordinary customers becomes a challenge, mainly due to the lack of broadband home networks with Quality of Service (QoS) provisioning [18].

Ethernet is often suggested by service providers, but for the vast majority of existing houses, Category 5 or higher Ethernet cables with Structured Wiring are not available. Retrofit or rewiring turns out to be very expensive, and running cables along corners or outside houses is also very awkward. Both service providers and customers are looking for alternatives. Several industry groups prompt the so-called “no-new-wires” technologies to transport Ethernet frames over existing household cable, phone and power wires, but their availability and achievable performance are still quite uncertain, and the wires may not be conveniently connected to video devices [19].

Whenever possible, consumers still prefer wireless solutions, evidenced by the proliferation of IEEE 802.11 Wireless Local Area Networks (WLAN), due to their availability, affordability and flexibility [20]. Even with the data rate increase in IEEE 802.11g/n and the QoS improvement in IEEE 802.11e, delivering high-quality video over WLAN with QoS guarantee still remains an open problem, especially in a household environment full of obstacles and interferers. Existing research reveals that the conventional single-hop wireless Access Point (AP) structure may not be sufficient to cover the entire house with satisfactory performance around every corner [26].

In addition, there are three kinds of WPAN technologies based on the data rate they are targeting on: IEEE 802.15.4 and Zigbee for low rate WPANs, IEEE 802.15.3 and Ultra-Wide Band (UWB) for high rate WPANs, and IEEE 802.15.1 and Bluetooth for the medium. Among these three, UWB is considered as the best technology for multimedia traffic, due to its high data rate (up to 480 Mbps in WiMedia UWB, potentially to Gbps), large bandwidth and low emission power [1] (i.e., less interference to other devices and more resilient to interference from others, which is preferred in a household environment).

In addition to the favorable physical-layer characteristics, WiMedia UWB also has some attractive features in its Media Access Control (MAC) layer. There are two kinds of MAC protocols supported: Prioritized Contention Access (PCA) and Distributed Reservation Protocol (DRP). PCA is extended from IEEE 802.11e Enhanced Distributed Channel Access (EDCA) function, with a contention-based, prioritized Quality of Service (QoS) provisioning. On the other hand, DRP is reservation-based and provides parametrized QoS, but unlike other reservation schemes, DRP allows devices to negotiate and reserve time slots without a centralized controller. Both features make UWB a primary candidate for IPTV in-home distribution, since video traffic usually has a high-bandwidth and low-delay and jitter requirement, and will

need both PCA and DRP due to its highly variable data rate.

In this research, we have first constructed a small UWB testbed using commercially available products in order to evaluate the feasibility and performance of high quality video streaming over UWB networks. However due to the limitations in commercially built products, we could only do experimentation on distributed reservation protocol of UWB MAC. By carefully choosing the experiment scenarios to represent a typical household environment, we identify the intrinsic tradeoffs in UWB physical and MAC layers with regard to transmission rate (TxRate), retry limit, reservation percentage and pattern. For a given channel condition, a suitable TxRate and retry limit have to be chosen for high throughput and reliability. To reduce the turnaround overhead for high throughput, clustered reservation is preferred; on the other hand, to reduce the service interval for low latency, a scattered reservation is better.

Furthermore, to extend the research to generic scenarios, we used both performance analysis and network simulation approaches to study the throughput and video streaming performance of UWB wireless networks. We follow the renewal reward theorem approach used in [2] to analyze the performance of WiMedia UWB PCA in both saturated and unsaturated cases, without or with the presence of DRP. We focus on the frame service time, i.e., the time from the instance when a PCA frame starts to contend for the channel to when the frame is transmitted successfully or dropped due to reaching the retry limit, and the achievable throughput can be derived accordingly. Frame service time is of particular importance to delay-sensitive applications such as video streaming.

In addition, we extend the Network Simulator (NS-2) [17] to support WiMedia MAC with UWB-specific physical-layer parameters, and the simulation results have indicated the efficacy of the analytical models and the ways to better support video traffic. Using this extended tool, we evaluated the application-oriented performance

metrics such as Peak Signal-to-Noise Ratio (PSNR) and frame delay/jitter for video streaming over UWB networks. To prove again the superiority of UWB we have presented video streaming performance considering all UWB MAC specific parameters - soft DRP, hard DRP, TXOP etc.

The contributions of this thesis have three aspects. First, we built a UWB wireless testbed using commercially available products. To the best of our knowledge, this is the first work reported in the open literature on the performance of video streaming over UWB networks with an experiment-based, application-oriented approach. Second, we build and improve in both accuracy and coverage a set of analytical models for WiMedia UWB MAC with both PCA and DRP. Although the renewal reward theorem has been employed before, no such models have been built specifically for WiMedia UWB so far. Third, this is the first time such models are validated with a commonly-used network simulator, other than just numerical calculation and in-house simulation. The models and the simulation code base provide an opportunity for the research community to further explore the performance and improvement of UWB MAC protocols.

The rest of the thesis is organized as follows. In Chapter 2, we review the current state-of-the-art approaches in IPTV in-home distribution, and summarize the related work on UWB experimentation, MAC layer analysis of UWB and other wireless technologies in Chapter 3. In Chapter 4, we present our UWB wireless testbed and video streaming experimentation. In Chapter 5, we present our analytical model and the detailed frame service time analysis method of UWB MAC. In Chapter 6, we first validate our analytical and simulation models by calculation and *NS-2* simulation, then we evaluate the performance of video streaming over UWB wireless scenarios in simulation considering all special features of UWB. In Chapter 7, we summarize our overall achievements in this research and discuss the ways to further improve video



streaming quality.

## Chapter 2

# Background

Wireless technologies get popular as people's vision of having Internet anytime anywhere becomes widespread. In some places WLAN and WMAN technologies are deployed to act as the access network of the Internet to keep the Internet services going in each and every corner of the world. One of the most attractive and popular Internet services is IPTV whose demand is increasing due to the invention of high bandwidth affordable broadband access network.

In addition, wireless technologies are very attractive for in-door communication systems due to their convenience, flexibility and increased affordability, evidenced by the popularity of cordless phones and WLANs. IPTV and other whole-house entertainment applications such as Personal Video Recorder (PVR) further drive the need for video streaming over short ranges in a household environment, with WLANs and WPANs as two main candidates for cross-room and in-room scenarios. However, wireless video streaming is much more challenging due to its high bandwidth, low delay and jitter requirement.

In this chapter we want to give an overview of the materials relevant to this research. First we will briefly introduce the popular WLAN technology IEEE 802.11

followed by existing WPAN technologies. Our research focus UWB wireless technologies will be discussed in the next section and finally we will explain issues relevant to video streaming over wireless networks.

## 2.1 IEEE 802.11 WLAN

Currently, IEEE 802.11 [20] is the dominant technology for WLAN due to its low cost, easy deployment and high flexibility. Most portable devices now have WLAN interfaces embedded to support one or more modes of IEEE 802.11a/b/g. In theory, IEEE 802.11b can support raw data rate up to 11 Mbps and 802.11a/g up to 54 Mbps, which appears to suffice for high-quality video streaming. However, due to the high overhead in IEEE 802.11 physical and MAC layers, less than 50% of the raw data rate is available to the application layer. Newer technologies, such as IEEE 802.11n, are emerging, but they are still at a very early stage and not widely available yet, so here we just discuss IEEE 802.11a/b/g.

In a household environment, cross-room wireless signals are attenuated and reflected by floors, walls, doors and moving objects such as human beings and pets, which reduces the received signal strength. Also, IEEE 802.11 devices are working in the same 2.4 and 5 GHz unlicensed frequency bands as other home appliances such as cordless phones and microwave ovens, which introduces interference and further reduces the received Signal-to-Noise Ratio (SNR). Given the limited number of channels available, it is not unusual to see IEEE 802.11 devices working in a low SNR condition with limited capacity. [26] points out that the average throughput of IEEE 802.11g devices in a household environment is about 10 Mbps due to high attenuation, interference and shadowing, which makes it less ideal for high-quality video streaming, especially with multiple video streams.

IEEE 802.11 MAC, even in 802.11n, is mainly based on Carrier Sense Multiple Access with Collision Avoidance (CSMA/CA), and each device has equal probability to access the channel. Due to channel contention, devices are constrained by the one with the lowest data rate, and some devices have to wait a relatively long time to access the channel [19]. Obviously, contention-based MAC is not suitable for real-time applications such as IPTV that have stringent delay and jitter requirements. Contention-based MAC also reduces achievable throughput due to channel idle and collision times. IEEE 802.11e Enhanced Distributed Channel Access (EDCA) [20] is proposed to prioritize channel access and targets at multimedia applications. However, EDCA is a statistical priority scheme and cannot guarantee the performance for high priority traffic and may starve the low priority one.

## 2.2 IEEE 802.15 WPAN

For wireless personal area networks, IEEE 802.15 working groups specify a number of standards. Among which IEEE 802.15.1 and 802.15.4 are quite popular. Both standards can support low data rate at approximate 10 meters distance. IEEE 802.15.1 defines a protocol specification based on Bluetooth. Detailed PHY and MAC protocol specifications of this family have been described in [59, 57]. There are two kinds of MAC layer operating modes supported in IEEE 802.15.4 standard: an ad-hoc non beacon enabled mode and a beacon enabled mode. Ad-hoc non beacon enabled mode follows CSMA/CA (Carrier Sense Multiple Access with Collision Avoidance) mechanism to compete for the channel access. If the channel is idle, transmission is started immediately, otherwise stations go for backoff and try to access later. Beacon enabled mode is also the MAC layer specification for IEEE 802.15.1 standard. According to the beacon enabled mode, time is divided into superframes. A superframe consists of

two parts: Contention Free Period (CFP) and Contention Access Period (CAP). In the CFP mode, network coordinator alone controls all contention free channel access by assigning guaranteed time slots to individual nodes. The assignment of guaranteed time slots to individual nodes is performed by the centralized coordinator with some scheduling mechanisms that have been extensively studied in the literature [58, 56]. In the contention access period, nodes usually access the channel with the CSMA/CA mechanism. Even though with the prioritized contention access mechanism, the highest priority traffic (multimedia traffic) can be given a higher access priority by assigning some configurable parameters, guarantee of QoS is still unexpected. To guarantee the QoS requirement in personal area networks, contention free period seems to be the hope. However, these standards require an centralized co-coordinator to maintain communications among all nodes in the networks.

## 2.3 Ultra-Wide Band Technologies

UWB is a radio technology that can be loosely defined as any wireless transmission schemes with bandwidth more than 25% of its center frequency, or more than 500 MHz [28]. There are two camps of UWB, DS-UWB and MBOA-UWB. DS-UWB, referred to as Direct Sequence UWB, is based on Direct Sequence Spread Spectrum (DSSS) technology. MBOA-UWB, which eventually became WiMedia UWB, is based on the combination of Time-Frequency Coding (TFC) and Orthogonal Frequency-Division Multiplexing (OFDM) technology. Here we focus on WiMedia UWB as it now becomes commercially available off the shelf.

UWB has a few unique features to make it a better candidate for high-quality video streaming: ultra wide band, high data rate, and low power emission. WiMedia UWB uses a 528 MHz band with TFC hopping in the 3.1 to 10.6 GHz frequency

range, which enables many more channels than IEEE 802.11 to accommodate more device groups. With such a wide band, WiMedia UWB can support raw data rate up to 480 Mbps and potentially to 1,000 Mbps, even with a lower SNR. By transmitting at a very low power level, UWB has very little interference to other devices, and is less susceptible to interference from other devices as well. Low power consumption also means better energy conservation for battery-powered portable consumer electronics.

In addition to the physical layer features mentioned above, UWB MAC has its own features to further benefit high-quality video streaming. WiMedia [16] has two types of MAC schemes: Distributed Reservation Protocol (DRP) and Prioritized Contention Access (PCA). Time duration in WiMedia MAC is equally divided into superframes of 65 ms each, and each superframe has 256 Medium Access Slots (MAS). The first 32 slots can be used for Beacon Period (BP), during which each UWB device can broadcast and inform others about the slots in the following Data Transfer Period (DTP) it reserves for exclusive access. Consequently, in the reserved slots, the “owner” device transmits at the beginning of the slot without contending for the channel, and others have to wait for their reserved slots. DRP provides guaranteed access and performance. For unreserved DTP slots within the same superframe, each device contends for the channel with PCA. PCA is similar to EDCA with prioritized channel access. In the next section an overview of EDCA is given.

## 2.4 Overview of IEEE 802.11e

Since one of the data transfer period protocol of UWB MAC, PCA is similar to IEEE 802.11e MAC standard or EDCA, in this section we want to briefly explain how traffic prioritization is maintained in this protocol. In fact the way of channel access of PCA or EDCA protocol is similar to IEEE 802.11 DCF, however DCF is for

homogeneous networks where all traffics have the same statistical chance to access the channel. Usually IEEE 802.11 LANs use the basic access mode instead of the RTS/STS mechanism and the focus of our discussion in this section is based on the former. The latter is applicable when the packet size in the MAC sublayer is larger than some threshold value.

In PCA protocol, user traffic is differentiated according to different parameters: minimum contention window size, maximum contention window size, arbitration interframe space and TXOP (Transmission Opportunity) value. Higher priority traffic is assigned lower values of these all parameters to get a higher priority to access the channel. When a frame comes from the upper layer, the MAC layer first senses the channel. If it finds the channel is idle, first it keeps silent for an AIFS period of time and then transmits the frame. If the channel is busy when a frame comes, that particular station keeps silent for an AIFS period of time after the channel becomes idle and then starts its backoff counter decrementing procedure. When the duration of AIFS is expired, it decrements its backoff counter ahead of the time slot no matter the channel is busy or idle. In our work we have differentiated two priority traffic  $AC_1$  and  $AC_2$  by varying the parameters including minimum contention window size, maximum contention window size and AIFS. For the simplicity of the analysis we have considered only two kinds of user traffic exist in the system. Since the AIFS value of two priority traffic is different we have divided the channel access region into two zones  $Z_1$  and  $Z_2$ . The length of  $Z_1$  is the AIFS difference between two traffics. In  $Z_1$  only  $AC_1$  stations contend for the channel whereas in  $Z_2$  both priority traffics.

## 2.5 Video Streaming over Wireless Networks

Recently H.264 encoded video gets huge popularity due to its quality and compression scheme. Another name of this standard is MPEG-4 Part 10 or MPEG-4 AVC (Advanced Video Coding). This standard is capable of providing good video quality at substantially lower bit rates than previous standards (e.g, half or less of the bit rate of MPEG-2, H.263, or MPEG-4 Part 2), without increasing the complexity of design and implementation. One of the extensions of this standard is FExt (Fidelity Range Extension) enables higher quality video coding with increased precision and higher resolution. The quality of a video encoded by this standard is the same with a data rate of 2 Mbps when compared with the video encoded by MPEG-2 standard with a data rate of 12 Mbps. However the peak to average data rate ratio of this standard is pretty high compared with other standards. Therefore it introduces more challenges on the transmission of video compressed by this scheme due to its sensitive nature to the loss of packets.

In this research we have applied H.264 encoder on a raw 2 minutes HD camera demo video clip. Since the resource of wireless channel is scarce, the transmission of H.264 encoded video incurs more challenges due to the high data variability of this encoding scheme. The focus of our research is the UWB wireless technology that has very high data rates and includes special MAC layer protocols which are very suitable for the transmission of such highly compressed video data without sacrificing quality of the video. The main point of this thesis is to investigate how these special physical and MAC layer features of UWB wireless networks work with the transmission of H.264 encoded video.



## Chapter 3

# Related Work

In this chapter, first we review the existing work on UWB experimentation. Then the analysis work of contention based MAC and TDMA or DRP MAC is presented in the subsequent paragraphs. Finally we will illustrate the work done on UWB MAC analysis.

There are a few efforts reported in the literature on UWB prototyping and experimentation, but they mainly focus on the physical layer with proprietary software for demo purpose. For example, [29] presented a wireless display system to transport raw, uncompressed analog video signals through UWB from a smartphone to a data projector. [30] implemented a UWB-based wireless communication system using multi-FPGA hardware and discrete RF design to achieve a maximum data rate of 110 Mbps.

There are various techniques reported in the literature for the analysis of IEEE 802.11 MAC, notable among which are equilibrium point analysis, mean value analysis, and Markov chain analysis. Previously there were some works have been done on the analysis of CSMA-based MAC using equilibrium point analysis [9]. For example, Wang proposed an analytical model for IEEE 802.11 DCF using equilibrium

point analysis under the unsaturated traffic condition [9]. However as the number of station is increased and the complexity of this protocol is increased this mechanism is not efficient to apply. After that Markov chain model gets more popularity due to its flexibility to analyze some CSMA/CA based protocols. Bianchi first proposed a discrete time Markov Chain model to obtain the saturated throughput of the Distributed Coordination Function (DCF) in IEEE 802.11 [4]. Following that, several papers appeared to extend Bianchi's model. Ziouva and Antonakopoulos improved Bianchi's model to derive the saturated delay [5]. Wu et al. improved Bianchi's model to consider the retry limit [6]. Xiao and Rosdahl studied the maximum throughput and its limit [7]. Medepalli's IEEE 802.11 throughput analysis used an average cycle time approach [8].

All of those analysis efforts discussed above are for homogeneous network, do not capture the behaviour of a network where multimedia traffic is given a higher priority to access the channel. Several priority studies have been reported in the literature for the DCF. Deng and Chang [38] proposed a priority scheme by differentiating the backoff window. Veres et al. [39] proposed priority schemes by differentiating the initial backoff window size and the maximum window size. Aad and Castelluccia [40] proposed a priority scheme by differentiating interframe spaces (IFS). Pallot and Miller [41] proposed an interesting prioritized backoff time distribution mechanism in which the backoff time is chosen in the current window range with different distributions for different priorities. All the priority schemes [4, 5, 6, 7] were based on simulations. Xiao [7] proposed an analytical model to evaluate backoff-based priority schemes by differentiating the initial window size, the backoff window-increasing factor, and the maximum backoff stage.

To support MAC-level QoS, the new amendment of IEEE 802.11 becomes standardized and is called as IEEE 802.11e. Robinson proposed a discrete time Markov

chain model to obtain the saturated throughput for the Enhanced DCF (EDCF) in the draft 802.11e [10]; in addition, he also considered the post-backoff waiting period in his model. Around the same time, Kong developed an analytical model of IEEE 802.11e EDCA [11], taking into account different AIFS periods, contention window sizes and virtual collision. Performance analysis of 802.11e by Xiao is another example [12]. EDCA analysis under the unsaturated condition came out recently by Engelstad [13]. His model can predict throughput and delay under the range of light to saturated traffic load by adjusting various parameters.

One of UWB MAC protocols is the distributed reservation protocol or DRP. This protocol is fundamentally similar to existing TDMA-based reservation protocols. However through TDMA reserved time slots have some constraints, for example, 1) single slot per station per cycle, 2) multiple continuous slots per station per cycle. Here the cycle concept is similar to the superframe in UWB MAC. In the literature, the centralized TDMA protocol and its variants have been extensively studied [48, 49, 50]. Due to these constraints QoS (delay performance) obtained for multimedia traffic is not flexible and practical. Distributed reservation protocol or DRP is able to give better delay bound since reserved time slots can be distributed across the superframe. Recently one work [33] proposed a two dimensional discrete time markov chain model to capture the delay bound when reserved time slots follow the distributed reservation protocol. Since the available slots for reservation may be arbitrarily located in superframe, reservation pattern can be arbitrary. In our experiment we have investigated the impact of reservation patterns on the protocol performance in terms of throughput and delay. Arbitrary reservation patterns also affect the performance of PCA protocol since the time slots available for PCA become also random when the reserved time slots are arbitrary. Through analysis and simulation we have seen how the PCA performance is affected by different percentage and pattern of reserved time

slots.

The emergence of UWB also attracted attention recently due to its superiority for multimedia traffic, and quite a few research work has been done on the analysis of WiMedia UWB MAC. Wong first analyzed the UWB MAC considering DRP, beacon period and PCA [14]. His model is built on the top of a discrete time Markov chain, but he only showed the numerical throughput results for PCA with saturated traffic and did not have simulation or experimentation-based validation. Recently, a renewal reward theorem-based approach is proposed by Ling et al. to analyze EDCA-like MAC [2], but his analysis just considered PCA without DRP. In addition, he only verified his model with in-house simulation. Due to the time difference of AIFS periods between two priority classes, the pre-backoff waiting period for the lower priority traffic is largely overestimated in his model. Motivated by our experimentation work [15], we further improve their model in many aspects and verify the accuracy by using a well-known network simulator, NS-2. We also derive the frame service time for both saturated and unsaturated traffic with the presence of DRP.

## Chapter 4

# Experimentation

As discussed in Chapter 2 and Chapter 3 for IPTV in-home distribution wireless technology is a better solution. In this thesis, we want to investigate the performance of UWB wireless technology as an IPTV in-home distribution solution.

Due to the broadband access networks, IPTV service is now at the doorstep. Through the wireless access router this service is now in a particular room. Now the question is, how to distribute this video stream to TV, DVD or handheld devices. As we argued a lot in the previous few chapters, UWB is the best technology for the transmission of high quality video streams. UWB supports very high data rate in 10 metres distance, at the same time its MAC layer supports two protocols: Prioritized Contention Access (PCA) and Distributed Reservation protocol (DRP). Both of these protocols support the transmission of high-quality video streams with possible QoS provisioning. Distributed reservation protocol allows each station or device to have guaranteed channel access with a proper delay bound. Motivated by these features of UWB, we have done some experimentation on commercially available UWB products. Content of this chapter has been disseminated in our paper [15].

The rest of the chapter is organized as follows: the way on how the performance

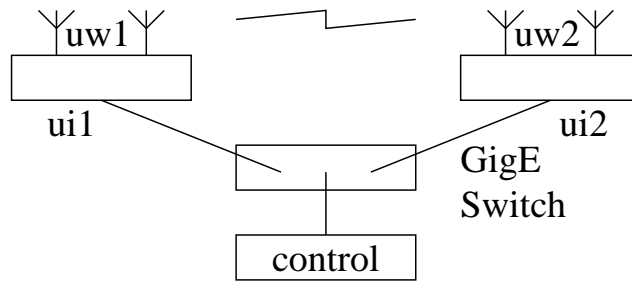


Figure 4.1: Testbed Configuration.

evaluation is done is described in Section 4.1, followed by the performance analysis of distributed reservation protocol in Section 4.2, and the experimentation results are described in Section 4.3.

## 4.1 Evaluation Methodology

In this section, we first give a brief outline of our testbed configuration, and then illustrate the performance metrics of our interest and the approaches to obtaining them.

### 4.1.1 Testbed Configuration

As shown in Fig. 4.1, our testbed has two UWB nodes referred to as **uw1** and **uw2** with Tzero ZeroWire Mini PCI 700 Revision B card and dual antenna [35]. Tzero firmware (tz7110), host driver (Version 3.3.10), configuration (Version 1) and control software are used on these two nodes. Tzero configuration file allows us to manually select TxRate, retry limit and receiver diversity (RxDiversity), and set reservation percentage and pattern. By experimenting with the reservation map, we have confirmed that we can reserve with arbitrary percentage and pattern. Also, each node has a Gigabit Ethernet link for control purpose, which allows us to remote access them without affecting with ongoing tests.

These two UWB nodes are about 10 meters away in a line-of-sight setting. In order to emulate a household environment full of obstacles and interference, we used two tea cans to cover `uw2`'s antenna for a resultant Received Signal Strength Indicator (RSSI) around -73 dBm, which appears to be background noise for non-UWB devices. We select channel 14 (TFC 6), which is a fixed frequency interleaving at 3.96 GHz, TxRate among 53.3, 80, 106.7, 160, 200 and 480 Mbps, retry limit from 0 to 7, and automatic RxDiversity. Unless otherwise stated, we use the so-called latency schedule with close to 50% slots reserved for `uw1` and `uw2`, respectively, and we set reservation patterns with different scatter levels through the configuration file.

However, there are some limitations in our experimentation. First, not all WiMedia data rates, even the mandatory one at 300 Mbps, are supported by the Tzero cards in our testbed. Since the supported data rates use both QPSK and DCM modulation, we believe our testbed is representative for other missing data rates with the same modulation scheme. Second, our cards have a limited support on DRP and no support on PCA: if a slot is not reserved by either `uw1` or `uw2`, the slot is not attempted with PCA, even when both `uw1` and `uw2` have data to send; if a slot is reserved by both `uw1` and `uw2`, they will attempt to send packets in the same slot, which results in collision. Since we focus on DRP-supported video streaming, we can arrange the reservation map on `uw1` and `uw2` properly to avoid under or over utilization. Third, in addition to the first 32 slots reserved for BP, the last 16 slots, if reserved, will break the connection between `uw1` and `uw2`. We believe this is an implementation issue of Tzero cards, so we can reserve at most 208 slots for `uw1` and `uw2`, or 104 slots each with the 50% reservation.

### 4.1.2 Network Characterization

In order to evaluate the DRP capacity at a given TxRate, retry limit, reservation percentage and pattern, we need to first find out how many packets can be sent out and received in one superframe by  $uw1$  and  $uw2$ , respectively. We use throughput to denote the capacity achieved by the sender and limited by the reservation, and we use goodput to denote the capacity achieved by the receiver, taking into account TxRate and retry limit. By increasing the offered load, we can obtain the saturated throughput, which gives an upper bound of the performance achievable for video streaming.

We used D-ITG for network performance analysis [36]. D-ITG has a sender-receiver-logger structure to provide both sender and receiver traces at packet level. Given the high data rate of UWB, it requires very high precision of time synchronization if we want to obtain one-way delay. Instead, we instruct the application-layer acknowledgment of the data packets from  $uw1$  to  $uw2$  to return back to  $uw1$  through the Gigabit Ethernet control link and obtain the round-trip time. In fact, we have modified D-ITG to take additional arguments to transport all signaling and acknowledgment packets through the control link, so these packets will not affect the data packets sent through the UWB link under the test.

### 4.1.3 Video Evaluation

In our experiments, we used a two-minute high-definition video camera demo video clip as an example. The video has a resolution of 1920\*1080 and refresh rate of 24 frames per second. We applied the MPEG-4 AVC reference encoder on the raw video. MPEG-4 AVC, also known as H.264, is the newest video coding standard and has been widely adopted for high-definition TV (HDTV) services. Figure 4.1.3 shows the frame size of our encoded sample video. From the figure, we can tell the average frame



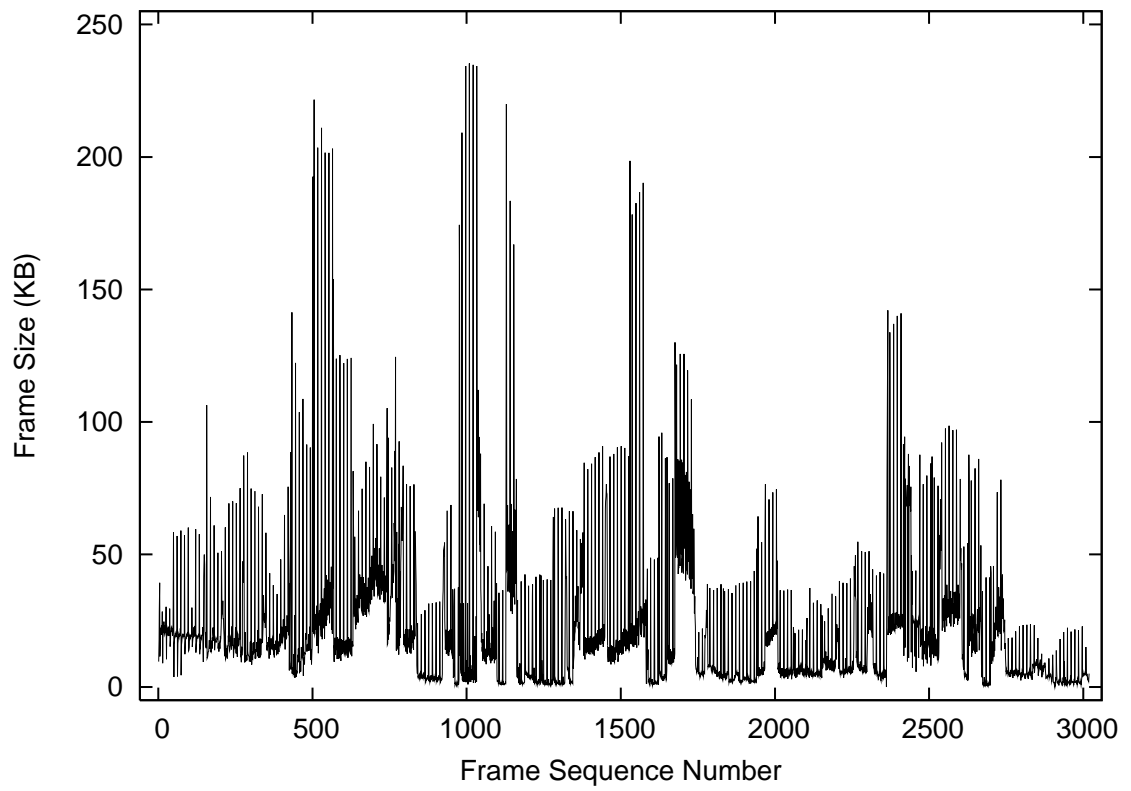


Figure 4.2: Frame Size vs Frame Sequence Number.

size is about 21.152 kilobytes. Average data rate can be obtained from the ratio of the average frame size and refresh rate. The figure also shows the high peak-to-average ratio due to the high efficiency of MPEG-4 AVC. We used multiple video streams to fully utilize the UWB link, e.g., four streams to represent quad-HDTV scenarios for cinema-like experience.

Video frames are further segmented in packets. MPEG-4 AVC employs a Group-of-Pictures (GoP) structure, and some frames (e.g., P or B-frames) are predicted based on others (I or P-frames). In this case, traditional network performance metrics such as packet loss and delay are not sufficient, since losing an I-frame will affect all frames in a GoP. To obtain application-level performance metrics, we used *EvalVid* [22] to capture the packet trace at both the video streaming server (**uw1**) and client (**uw2**). By comparing the sequence number and timestamp of each frame at both sides, we can calculate frame loss, delay and jitter. In addition, we can reconstruct the video stream with the received packets, and calculate Peak-Signal-to-Noise-Ratio (PSNR), which is regarded as an objective metric for video quality evaluation and also a good indicator for subjective ones for perceptual video quality evaluation.

## 4.2 Performance Analysis

In this section, we analyze the performance achievable by UWB at a given TxRate, by taking into account the protocol overhead in physical, MAC, logical link control (LLC) and upper layers. The analysis will be validated by the performance results given in the next section.

Video streams are often transported in Realtime Transport Protocol (RTP), which is consequently encapsulated in UDP, IP and LLC protocol with 8, 20 and 16-byte header, respectively, or for an overall overhead of 44 bytes above the MAC layer. In

WiMedia UWB, an OFDM symbol lasts  $T_{SYM} = 0.3125 \mu s$  and can carry a different number of information bits depending on modulation and coding schemes, which jointly determine the physical layer data rate. In the Physical Layer Convergence Protocol (PLCP), a standard or burst PLCP preamble of  $N_{sync} = 30$  or 18 symbols is prefixed for packet synchronization and channel estimation<sup>1</sup>, followed by a PLCP header of  $N_{hdr} = 12$  symbols. The remaining of the PLCP packet including a 4-byte Frame Check Sequence (FCS), a 6-bit tail and extra pad bit lasts an integer multiple of six symbols, which depends on the number of information bits per six OFDM symbols ( $N_{IBP6S}$ ) at the given data rate.  $N_{IBP6S}$  is 100, 150, 200, 300, 375 and 900 for 53.3, 80, 106.7, 160, 200 and 480 Mbps, respectively. Thus, if the UDP payload length is  $L$  bytes, the duration for the entire PLCP packet over the air in  $\mu s$  is

$$T = \{N_{sync} + N_{hdr} + 6 * \lceil \frac{(L + 44 + 4) * 8 + 6}{N_{IBP6S}} \rceil\} * T_{SYM}. \quad (4.1)$$

In a DRP reservation with no acknowledgment, PLCP packets are separated by a Minimum Inter-Frame Space (MIFS) of  $pMIFS = 1.875 \mu s$  if the burst mode is used or otherwise a Short Inter-Frame Space (SIFS) of  $pSIFS = 10 \mu s$ . The last PLCP packet in a DRP reservation should have a minimum guard time of  $mGuardTime = 12 \mu s$  before the end of the reserved slot, in addition to a SIFS regardless whether the burst mode is used. Therefore, for a DRP reservation covering  $n$  consecutive MAS slots of  $mMasLength = 256 \mu s$  each, the maximum number of PLCP packets can go through in the reservation is

$$N(n) = \lfloor \frac{mMasLength * n - mGuardTime}{T + pSIFS} \rfloor \quad (4.2)$$

---

<sup>1</sup>According to WiMedia specification, for data rates of 200 Mbps and lower, all the packets in the burst shall use the standard PLCP preamble; however, for data rates higher than 200 Mbps, the first packet shall use the standard PLCP preamble, while the remaining packets may use either the standard PLCP preamble or the burst PLCP preamble.

or

$$N(n) = \lfloor \frac{mMasLength * n - mGuardTime - \Delta}{T + pMIFS} \rfloor \quad (4.3)$$

with the burst mode, where  $\Delta = pSIFS - pMIFS$ .

## 4.3 Performance Results

In this section, we first present the network and video performance affected by TxRate and retry limit, and then we look further into the throughput-latency tradeoff affected by reservation percentage and pattern.

### 4.3.1 TxRate and Retry Limit

#### Packet Loss

Link-layer retransmission is an often-used technique to combat channel error. In our testbed, we can set a retry limit to determine how many local retransmissions are allowed before dropping a packet. In Fig. 4.3, we show the Packet Loss Ratio (PLR) with different TxRate and retry limit, when the reservation is at 50% with map {FF00}<sup>\*</sup>, which means only the first eight slots in every 16 slots are reserved for **uw1**. PLR increases with the increased TxRate at a given SNR. When the TxRate is 200 Mbps, the receiver cannot receive any packets due to the very low RSSI (-73 dBm) in our testbed and therefore PLR is 100%. On the other hand, PLR decreases with the increased retry limit due to local retransmission. When the TxRate is below 160 Mbps, the PLR is almost 0 with a non-zero retry limit. However, to facilitate local retransmission, the transmitter has to wait for the link-layer acknowledgment back from the receiver over the air and subject to channel errors, and retransmits when a timeout event occurs. As we shall see next, this waiting period also affects

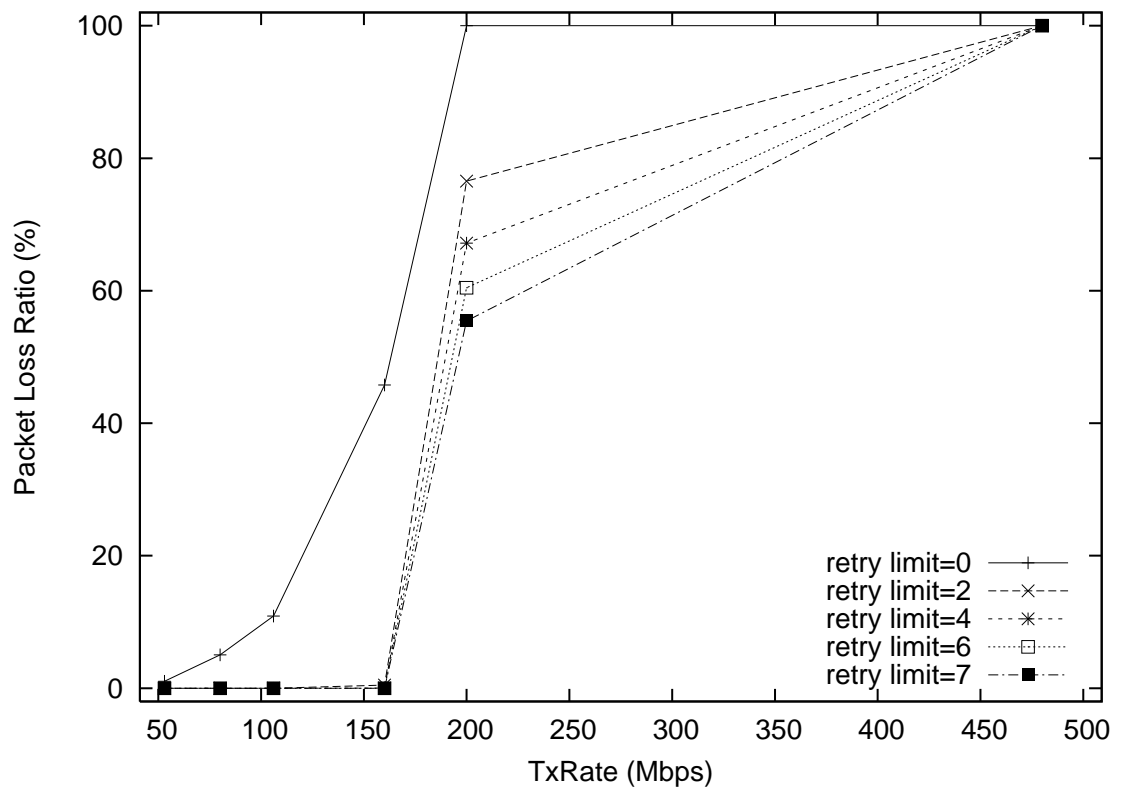


Figure 4.3: Packet Loss vs TxRate and Retry Limit.

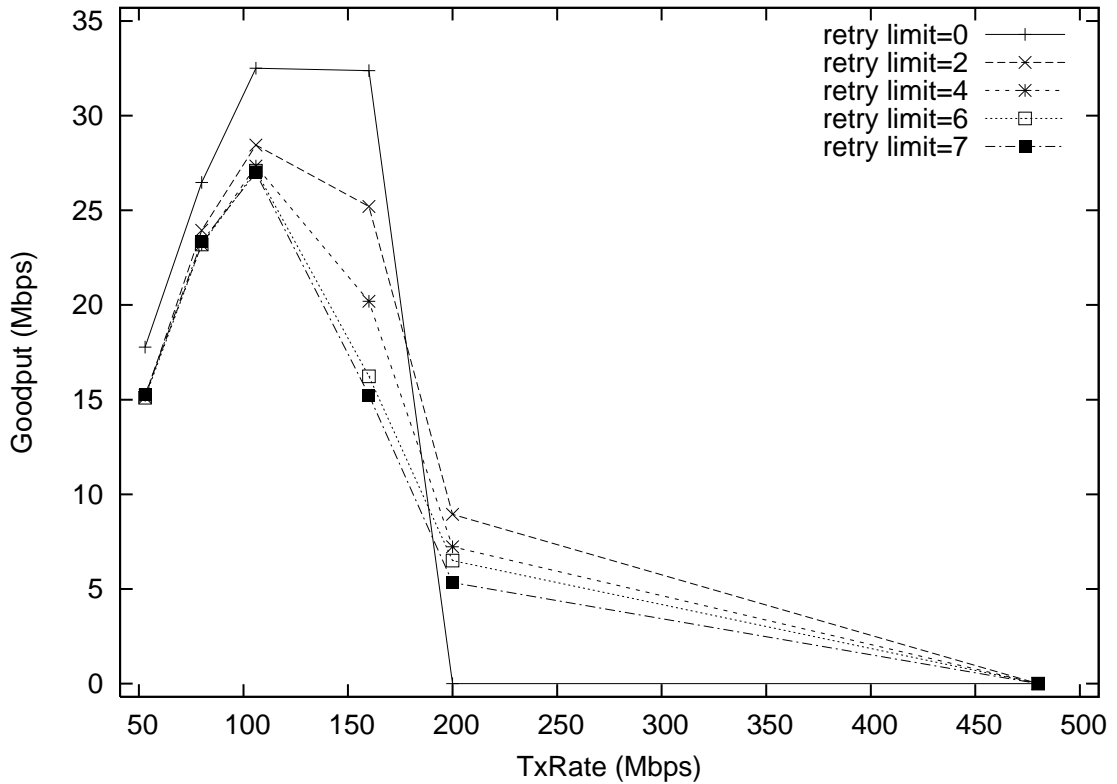


Figure 4.4: Goodput vs TxRate and Retry Limit.

achievable performance.

### Receiver's Goodput

In Fig. 4.4, we show the achieved goodput for different TxRate and retry limit. Goodput is determined at the receiver side depending on the throughput at the sender side and the PLR due to transmission error. When the TxRate is increased, packet transmission time is reduced, but the PLR is increased as shown in Fig. 4.3. Therefore, when TxRate is slightly increased, we see a considerable increase in achievable goodput. However, when TxRate is above a threshold (106.7 Mbps in our testbed), the increase in PLR is more significant, which greatly reduces the achievable goodput. When the TxRate is above 200 Mbps, the PLR is 100%, and the achieved goodput is 0. Figure 4.4 also shows that the increased retry limit actually reduces achievable

Table 4.1: Maximum Goodput (Retry Limit=0)

TxRate (Mbps)	Packets per Superframe	Goodput (Mbps)	
		Calculated	Measured
53.3	143	17.875	17.78
80	208	26.000	25.47
106.7	273	34.125	32.51
160	377	47.125	32.38
200	442	55.250	0
480	871	108.875	0

Table 4.2: Reservation Patterns

Index	Reservation Pattern for The Entire Superframe
1	0000 0000 CCCC CCCC CCCC CCCC CCCC CCCC CCCC CCCC CCCC CCCC CCCC CCCC CCCC 0000
2	0000 0000 FOF0 FOF0 FOF0 FOF0 FOF0 FOF0 FOF0 FOF0 FOF0 FOF0 FOF0 FOF0 FOF0 0000
3	0000 0000 FF00 FF00 FF00 FF00 FF00 FF00 FF00 FF00 FF00 FF00 FF00 FF00 FF00 0000
4	0000 0000 FFFF 0000 FFFF 0000 FFFF 0000 FFFF 0000 FFFF 0000 FFFF 0000 FF00 0000
5	0000 0000 FFFF FFFF 0000 0000 FFFF FFFF 0000 0000 FFFF FFFF 0000 0000 FF00 0000
6	0000 0000 FFFF FFFF FFFF FFFF 0000 0000 0000 0000 FFFF FFFF 0000 0000 FF00 0000

goodput, which seems counter-intuitive. This is due to the link-layer acknowledgment required for local retransmission, since the transmitter has to wait for the acknowledgment to come. For high-speed links such as UWB, such a waiting will keep the channel idle for a while in the reserved slots, which reduces channel utilization and eventually goodput. Therefore, block acknowledgment is necessary to improve both link utilization and reliability with retransmission. Unfortunately, block acknowledgment is not available through the existing configuration options for our Tzero cards.

The experimentation results in Fig. 4.4 have been validated by the goodput analysis results listed in Table 4.1, following (4.1)–(4.3). For a UDP packet with a 1024-byte payload, the total transmission time at 53.3 Mbps is  $174.375 \mu\text{s}$ . For a DRP reserva-

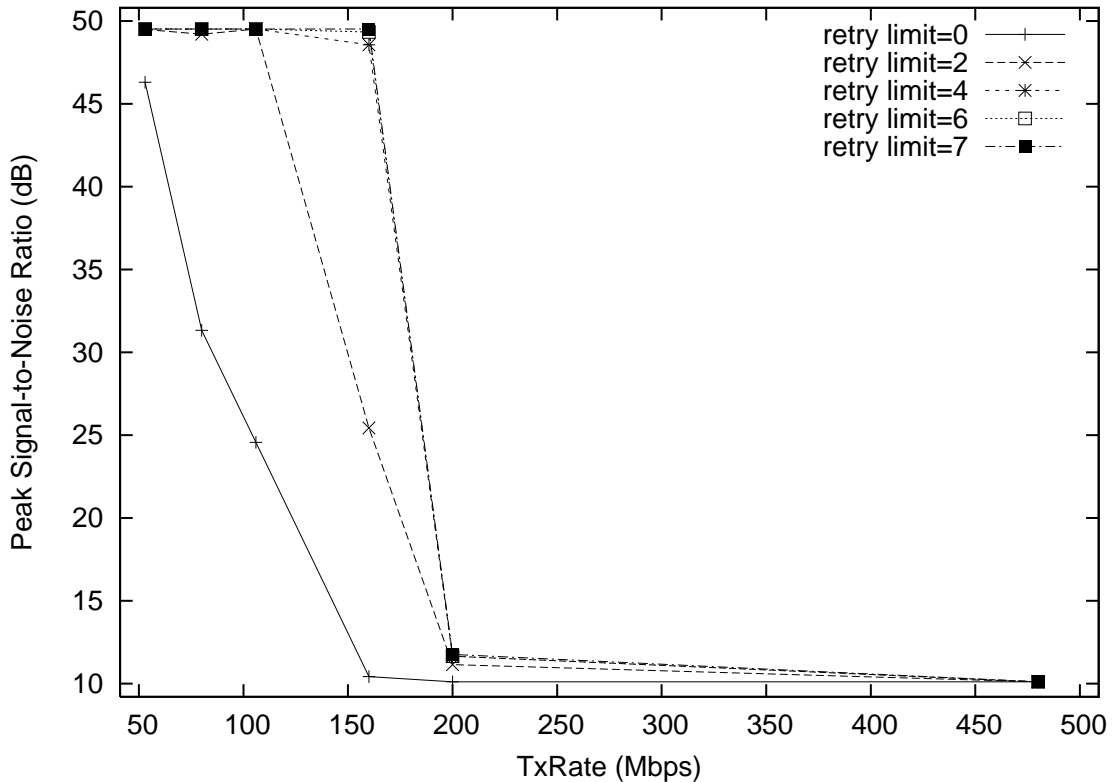


Figure 4.5: Average PSNR vs TxRate and Retry Limit.

tion without acknowledgment (i.e., retry limit = 0), the number of UDP packets can be transmitted within 8 consecutive MAS slots is

$$\lfloor \frac{256 * 8 - 20.125}{174.375 + 1.875} \rfloor = 11, \quad (4.4)$$

or 143 packets for the entire superframe with  $\{\text{FF00}\}^*$  reservation. Thus, the calculated goodput is 17.875 Mbps, while the measured one is 17.78 Mbps, as shown in Table 4.1. For TxRate higher than 160 Mbps, due to a higher packet loss ratio, the measured goodput is much lower than that predicted by the calculation assuming no packet loss.



## Video Quality

After obtaining the saturated goodput, we deliver video streams from **uw1** to **uw2**, and calculate frame loss, delay and jitter. With an increased TxRate, frame loss ratio (FLR) increases as well, due to the higher PLR at a given SNR. By reconstructing the received frames and comparing with the original ones, we can obtain the average PSNR. As shown in Fig. 4.5, the average PSNR decreases with the increased TxRate, due to a higher FLR. The higher the PSNR value, the better the reconstructed video quality, and a video stream of PSNR below 36 dB is considered not acceptable. As we can tell, local retransmission greatly improves link reliability and hence PSNR. In fact, with a retry limit of 7, the PSNR can achieve almost 50 dB when TxRate is below 200 Mbps between **uw1** and **uw2**, which is the upper bound for a lossy compression scheme such as MPEG-4 AVC. Given the almost-noise-like RSSI at **uw2**, this demonstrates the strong capability of UWB supporting high-quality video streaming in a household environment.

### 4.3.2 Reservation Percentage and Pattern

DRP is a unique feature in WiMedia UWB MAC and designed to support isochronous voice/video traffic. By reserving a certain number of slots for exclusive access in a superframe, a node is guaranteed to have a certain portion of link airtime, or the equivalent service rate. On the other hand, the gaps between these reserved slots determine the service interval. The service interval and queuing delay, which is determined by the service rate and the peak-and-average data rate, will further determine the access latency. In order to support high-quality video streaming, it is desired to achieve both high throughput and low latency at the same time with high channel utilization.

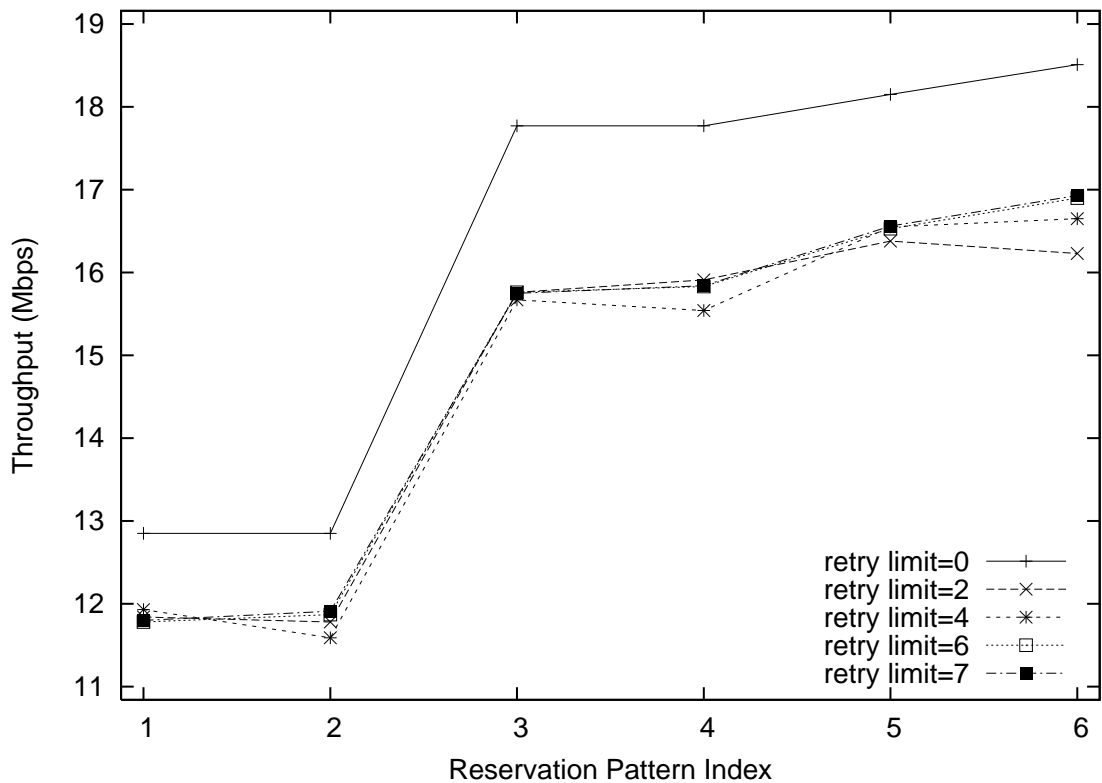


Figure 4.6: Throughput vs Reservation Pattern.

### Sender's Throughput

In order to show the effect of reservation patterns, we reserve 50% available slots with different cluster levels. For example, we can reserve every other  $2^i$  slots where  $1 \leq i \leq 6$  for a total of 104 slots, except for the last few dozens when  $i \geq 5$  as shown in Table 4.2.  $i$  is referred to as Reservation Pattern Index (RPI), and the higher the RPI is, the more clustered the reservation becomes. The RPI of our default reservation pattern  $\{\text{FF00}\}^*$  is 3. Figure 4.6 shows the achievable throughput with different retry limit and reservation pattern at 53.3 Mbps. As we can tell, when the reservations become clustered, due to the reduced turnaround overhead and guard time, the achievable throughput is increased. Again, due to the time for acknowledgment, the achievable throughput is reduced with a higher retry limit, corresponding

Table 4.3: Maximum Throughput (TxRate=53 Mbps)

Resv Index	Packets per Superframe	Throughput (Mbps)	
		Calculated	Measured
1	104	13.000	12.85
2	130	16.250	12.85
3	143	17.875	17.77
4	149	18.625	17.77
5	149	18.625	18.15
6	149	18.625	18.51

to the reduced goodput in Fig. 4.4. Even though in our experimentation we have reserved time slots in different patterns, we can reserve time slots arbitrarily across the superframe except first 32 and last 16 slots using the configuraion file.

The experimentation results in Fig. 4.6 have been also validated by the throughput analysis results in Table 4.3 as well, by following (4.1)–(4.3). At 53.3 Mbps and for RPI=1, every two consecutive MAS slots can accommodate

$$\lfloor \frac{256 * 2 - 20.125}{174.375 + 1.875} \rfloor = 2 \quad (4.5)$$

UDP packets with a 1024-byte payload, i.e., 104 packets in a superframe with {CCCC}\* reservation. Thus, the calculated throughput is 13 Mbps, while the measured one is 12.85 Mbps. Other reservation patterns show similar trends.

### Packet Delay

In Fig. 4.7, we show the packet delay affected by service interval for RPI 1 and 5, i.e., every other 2 and 32 slots are reserved, respectively. Since our objective is to show the delay caused by different reservation patterns, we have projected the time along the Y-axis and the sequence number along the X-axis. Note that the transmission and receiving time (Tx and Rx, respectively) curves are shifted horizontally to align with the start of a superframe at packet sequence number 104. The vertical time

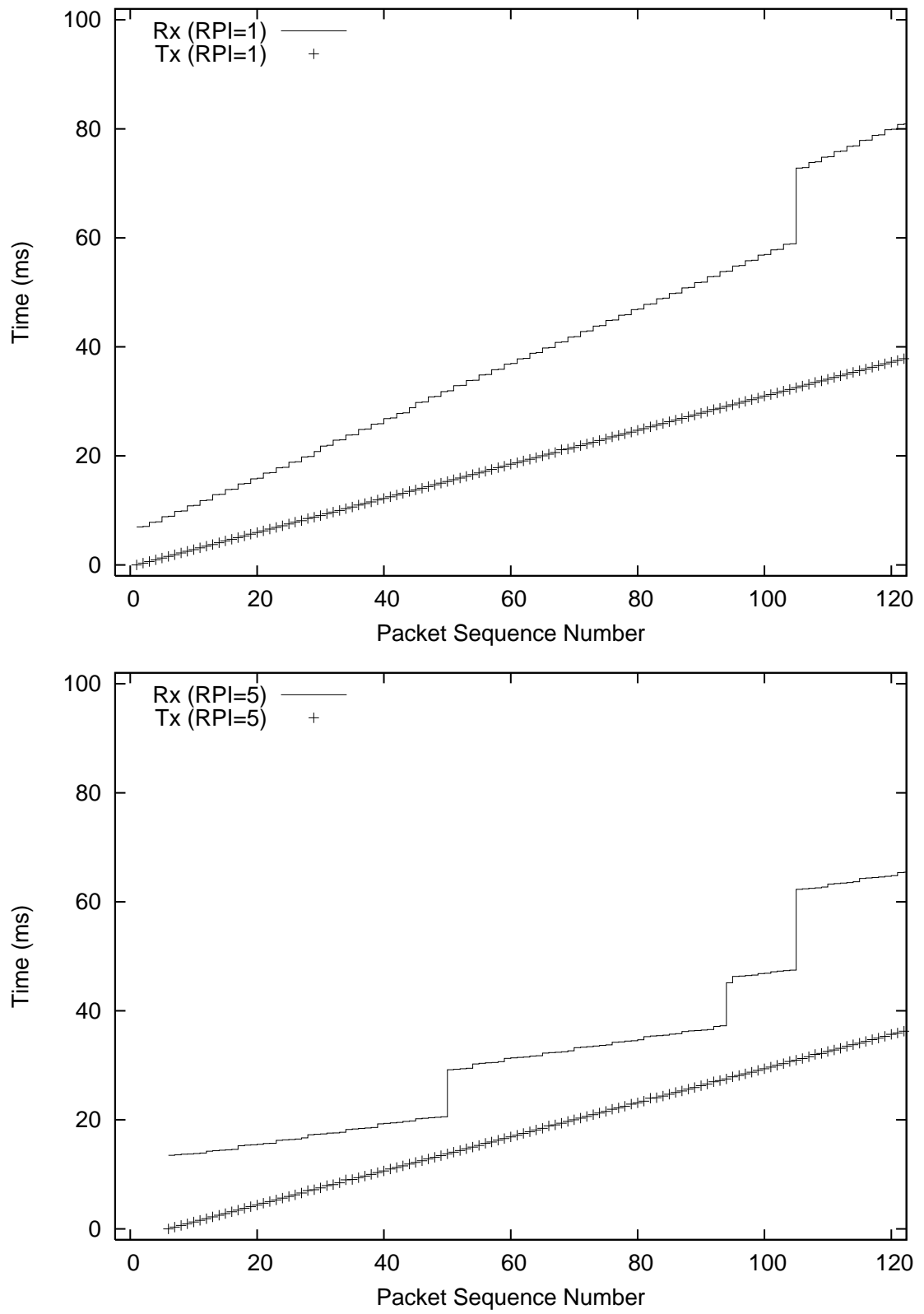


Figure 4.7: Packet Delay vs Packet Sequence Number.

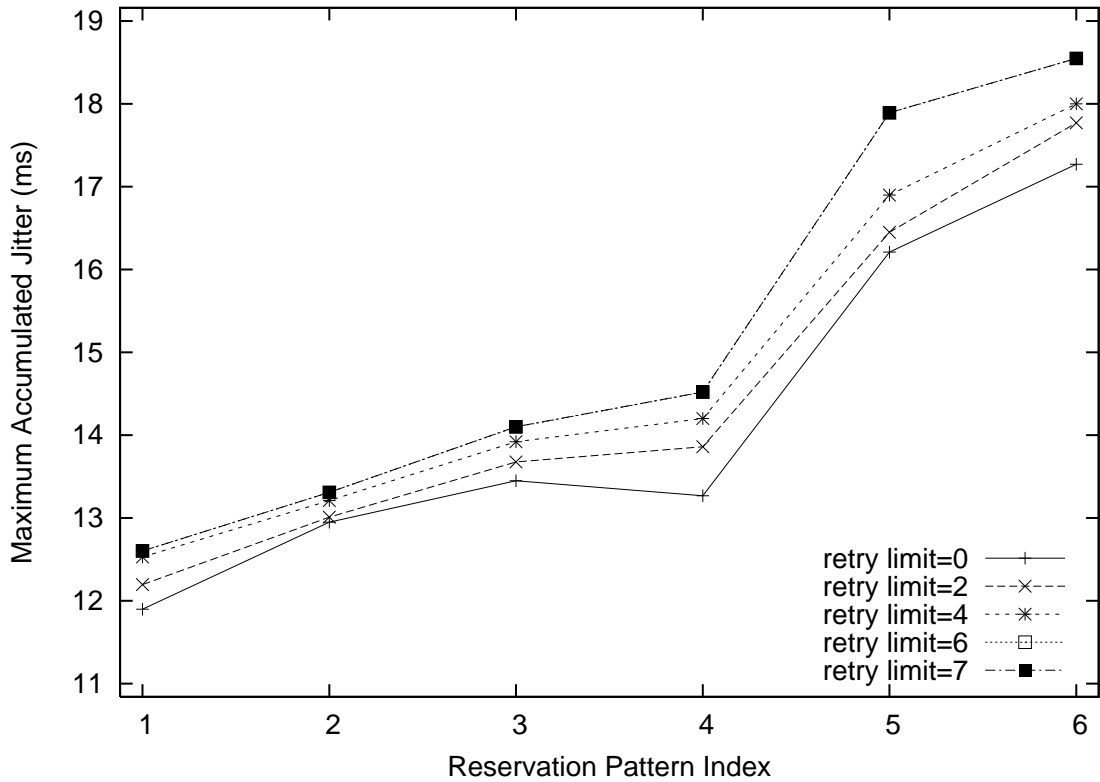


Figure 4.8: Frame Jitter vs Reservation Pattern.

difference between the Rx and Tx curves indicates the packet delay in round-trip time, which can approximate the one-way access latency due to the low, stable delay on Gigabit Ethernet. From the figure, we can tell packets are served regularly with small service interval when RPI=1. Due to the offered load (25 Mbps) is higher than this pattern can sustain (around 13 Mbps), we see an increased packet delay due to the increased queuing delay. When RPI=5, there are more packets served in the same time interval, indicating higher throughput; however, it suffers more obvious service interval that is longer than the case with RPI=1.

### Video Jitter

To further identify the effect of different reservation patterns on service rate and interval and consequently on access latency, in Fig. 4.8, we show the maximum ac-

cumulated jitter (MAJ) for the sample video. Frame jitter is defined as the time difference to deliver two consecutive frames, and is caused by the variation in service rate and interval. Again, the reservation is at 50%. As we can tell, when the reservations become clustered, due to the increased service interval, the MAJ is increased. The MAJ will determine the minimum initial buffering required to smooth the video playback. With an increased MAJ and given the high data rate supported by UWB, a much larger buffer is required to absorb the jitter and smooth the video, with a longer initial buffering time, which degrades video quality.

## 4.4 Summary

In this chapter, we have presented our UWB wireless testbed, which emulates a typical household environment. Due to the ultra-wide band, high data rate and low power emission, existing UWB devices can transport quad-HDTV or multiple HDTV video streams with satisfactory PSNR performance, even in our testbed where the SNR is very low. In addition, the MAC layer of UWB devices only support one protocol: Distributed Reservation Protocol (DRP), which allows guaranteed channel access and is suitable for high-quality video streaming with the given delay bound. To summarize, we have got two significant results: one is the tradeoff between TxRate and retry limit and another one is the tradeoff between two types of reservation patterns (clustered and scattered reservation patterns). At the given SNR, a higher TxRate means a higher packet loss ratio due to the different coding and modulation scheme. Whereas a higher retry limit causes a lower throughput due to the channel idle time and the time required to transmit the acknowledgement packet. The results obtained from different TxRate and retry limit help us to choose the optimal value of these two parameters so that a higher throughput is achieved, which is correlated to the

performance of HDTV-like high-quality video streaming. Distributed reservation protocol also introduces another tradeoff which is between different reservation patterns. From the results, we have observed clustered reservations are good to achieve higher throughput, however it introduces more delay which may affect the performance of high-quality video streaming. At the same time, scattered reservations reduce the delay while sacrificing the achievable throughput due to the guard time and more turnaround overhead. This experiment is just a case study. We have only developed one testbed emulating one household environment, however in future we can make a few more household environments to further evaluate the performance of UWB. We could not fully investigate UWB MAC in this case due to the limitations of commercially available UWB devices. Later on, we have generalized the evaluation of WiMedia UWB MAC through modeling and network simulation.

## Chapter 5

# Analytical Models

From the experimentation results, we have seen the performance of video streaming over the distributed reservation protocol. We have observed how reservation percentage and patterns affect the quality of video streaming in terms of PSNR, delay/jitter etc. Due to the limitation of our UWB devices we could not measure the video streaming performance over the PCA protocol of UWB MAC. Therefore in order to quantify the performance of video streaming we have developed an analytical model, which calculates the frame service time and throughput of the UWB PCA protocol from the low traffic load to the high saturated traffic load assuming there are no any DRP reserved slots in the superframe and then with the presence of DRP only for the saturated case.

As mentioned, we focus on *frame service time*, the time from the instance when a data frame becomes the head of the transmission queue and eligible to access the channel to when the frame is either transmitted successfully or dropped due to reaching the retry limit. For DRP, the frame service time is deterministic and bounded by the maximum DRP service interval, i.e., the gap between two consecutive DRP clusters, therefore, in this section, we only focus on the frame service time for PCA



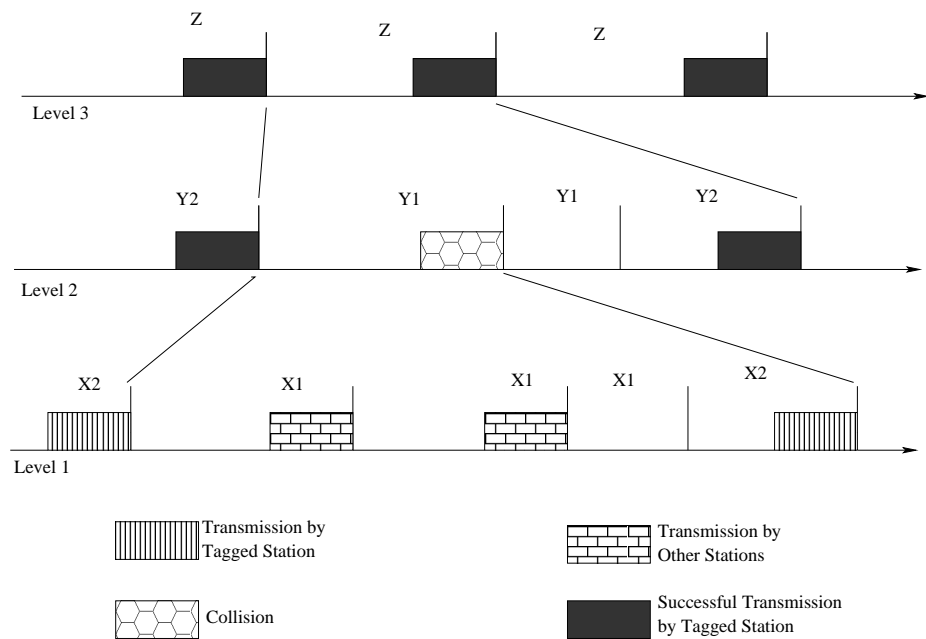


Figure 5.1: Renewal Reward Theorem

in saturated or unsaturated condition, without or with the presence of DRP. In fact when there are some DRP clusters in the superframe, the analysis of PCA becomes more challenging. Therefore first we present the analysis of UWB MAC when the entire superframe is used for PCA and then we put some DRP clusters and see the PCA performance with the presence of DRP. When the traffic is saturated, the achievable throughput is the ratio between the frame data payload length and frame service time, and when the traffic is unsaturated, the throughput is approximately the offered load.

The idea of this analytical model has been taken from the renewal reward theorem proposed by [2]. The basic principle of this theorem is presented in Figure 5.1. According to the figure, Level-1 cycle is the actual physical time to transmit one frame no matter the transmission is caused by the tagged station or other stations. Level-2 cycle is a number of transmissions by other stations followed by the transmission of the tagged station no matter the tagged station's transmission is successful or causes collision. Finally Level-3 cycle refers to a number of Level-2 cycles followed by the

successful transmission of the tagged station or the packet drop due to exceeding the retry limit. And Level-3 cycle is called the frame service time, a QoS parameter of video streaming and our interest as well.

To obtain the frame service time for PCA, first we have followed the approach used in [2] and then modified his model to capture the behavior of PCA after incorporating some DRP clusters interleaved with PCA. The network we have considered in this model is a piconet where every station can hear each other and there are no hidden terminal problems. Time is discretized into generic slots, which may have different lengths  $\delta$  or  $\Delta$ , depending on whether the channel is idle or busy (either successful transmission or collision). All the stations are assumed to be time-synchronized and they can correctly sense the channel at the beginning of a slot. Wireless channel is considered to be ideal, and transmission error only happens due to the collision caused by simultaneous transmissions from multiple stations. All MAC frames are assumed to have the same length and only two classes of traffic are considered (i.e.,  $AC_1$  and  $AC_2$ ). However, different frame length and more traffic classes can be incorporated in this analysis as well. For the ease of analysis at first we consider only one priority traffic exists per station and later we will show how the analysis will be modified when traffics of multiple priorities exist at each station.

The rest of this chapter is structured as follows. First we present our model when the whole time period is for PCA with saturated traffic followed by the model for unsaturated PCA, and finally the model considering DRP slots interleaved with PCA slots.

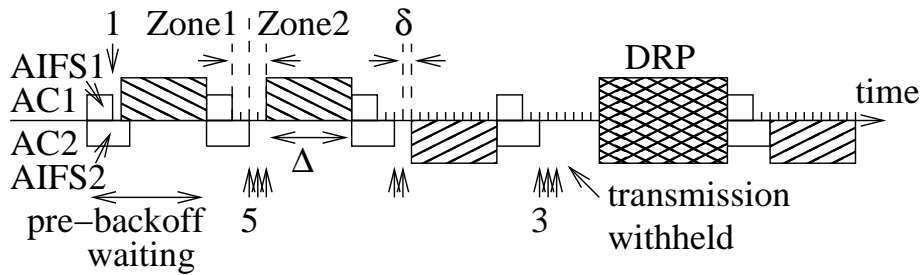


Figure 5.2: Prioritized Contention Access With The Presence of DRP.

## 5.1 Saturated PCA without DRP

As shown in Figure 5.2, there are  $N_1$   $AC_1$  stations and  $N_2$   $AC_2$  stations with Arbitration Inter-Frame Spacing  $AIFS_1$  and  $AIFS_2$ , respectively, where  $AIFS_2 - AIFS_1 = M\delta$ . According to the properties of EDCA,  $AC_1$  has higher priority and therefore has lower contention window size and lower arbitration inter-frame space. Between two AIFS periods, there are three possible scenarios:  $AC_1$  stations transmit in Zone 1 with probability  $\phi_{1,1}$ , where  $AC_2$  stations are still in their  $AIFS_2$  period;  $AC_1$  stations transmit in Zone 2 with probability  $\phi_{1,2}$ , where both  $AC_1$  and  $AC_2$  stations have finished their AIFS periods;  $AC_2$  stations transmit in Zone 2 with probability  $\phi_{2,2}$ . All major symbols used in the model are defined in Table 5.1.

In order to obtain the frame service time, we need to find two key probabilities: the transmission probability  $\tau_i$  and the conditional collision probability  $P_i$  for  $AC_i$  stations.

If a station experiences on average  $E[B_i]$  of backoff slots and  $E[R_i]$  transmission attempts, it has to pass  $E[B_i] + E[R_i]$  of generic slots to have one successful transmission. Therefore according to the the renewal reward theorem, in a randomly chosen slot, the transmission probability  $\tau_i$  of an  $AC_i$  station can be obtained as the average reward during the renewal cycle, given by

$$\tau_i = \frac{E[R_i]}{E[R_i] + E[B_i]}, \quad i = 1, 2. \quad (5.1)$$

Assuming an average collision probability of  $P_i$  for the frames of  $AC_i$  stations,  $R_i$  follows a truncated geometric distribution with MAC layer retransmission retry limit  $m$  and  $E[R_i]$  is given by

$$E[R_i] = \sum_{j=1}^{m-1} j P_i^{j-1} (1 - P_i) + m P_i^{m-1} = \sum_{j=0}^{m-1} P_i^j, \quad i = 1, 2. \quad (5.2)$$

Similarly,  $E[B_i]$  can be obtained as

$$E[B_i] = \sum_{j=0}^{m-1} (P_i^j (1 - P_i) \sum_{r=0}^j b_r) + P_i \sum_{j=0}^{m-1} b_j = \sum_{j=0}^{m-1} P_i^j b_j, \quad i = 1, 2 \quad (5.3)$$

According to the discussion above, an  $AC_2$  station can only transmit in Zone 2. Therefore, the average collision probability for a frame transmitted by the tagged  $AC_2$  station is given by

$$P_2 = 1 - (1 - \tau_1)^{N_1} (1 - \tau_2)^{N_2 - 1}. \quad (5.4)$$

For the tagged  $AC_1$  station, its transmission can occur in either Zone 1 or Zone 2, in which the contention situations are different. In Zone 1, only  $AC_1$  stations contend for channel access, while in Zone 2 stations from both classes contend. Therefore, the collision probabilities in Zones 1 and 2 are given by

$$P_{1,1} = 1 - (1 - \tau_1)^{N_1 - 1}, \quad P_{1,2} = 1 - (1 - \tau_1)^{N_1 - 1} (1 - \tau_2)^{N_2}. \quad (5.5)$$

To obtain the average collision probability  $P_1$ , we also need the probabilities  $\theta_i$  ( $i = 1, 2$ ) of a frame transmitted by the tagged  $AC_1$  station in Zone 1 or 2, respectively.

Table 5.1: Symbols Used in Model

m	Retry Limit
$P_i$	Collision Probability of $AC_i$ Station
$\tau_i$	Transmission Probability of $AC_i$ Station
$\phi_{i,j}$	Transmission Probability of $AC_i$ Station in Zone $j$
$\rho$	Station Busy Probability
$T_i$	Frame Service Time for $AC_i$ Station
a	Probability that Time Slot is Idle
b	Probability that Time Slot is Busy

Let  $M$  denotes the number of slots in Zone 1, which is the AIFS slot difference between  $AC_1$  and  $AC_2$  priority traffic. For a frame transmission from the tagged  $AC_1$  station, it occurs in Zone 2 only when neither itself nor any of the other  $AC_1$  stations transmits in the  $M$  consecutive slots in Zone 1 and it occurs with probability  $\theta_2$ . Therefore, we have

$$\theta_2 = ((1 - \tau_1)^{N_1})^M, \quad \theta_1 = 1 - \theta_2 \quad (5.6)$$

Thus, the average collision probability of an  $AC_1$  station is

$$P_1 = \theta_1 P_{1,1} + \theta_2 P_{1,2}. \quad (5.7)$$

From the above equations, the value of  $\tau_1, \tau_2, P_1$  and  $P_2$  can be obtained.

Then from the definitions of  $\phi_{1,1}, \phi_{1,2}$  and  $\phi_{2,2}$ , we get the following equation set

$$\phi_{1,1}/\phi_{1,2} = \theta_{1,1}/\theta_{1,2} \quad (5.8)$$

$$(\phi_{1,1} + \phi_{1,2})/\phi_{2,2} = \tau_1/\tau_2 \quad (5.9)$$

$$\phi_{1,1} + \phi_{1,2} + \phi_{2,2} = 1 \quad (5.10)$$

Solving these equations the values of  $\phi_{1,1}$ ,  $\phi_{1,2}$  and  $\phi_{2,2}$  can be obtained as well.

### AC1 stations

For a tagged  $AC_1$  station, on the average it spends  $E[Z_1] = E[R_1] + E[B_1]$  generic slots to service a frame. Among these generic slots,  $E[Z_1]\phi_{1,1}$  are in Zone 1 and  $E[Z_1](\phi_{1,2} + \phi_{2,2})$  are in Zone 2.

The average length of a generic slot in Zone  $j$  ( $j = 1, 2$ ) can be obtained by  $E[S_j] = a_j\delta + b_j\Delta_i$ , where  $\Delta_i = AIFS_i + T_{DATA} + SIFS + T_{ACK}$  for  $AC_i$  traffic.  $a_j$  and  $b_j$  are the probabilities of the channel being idle and containing a successful transmission or a collision in Zone  $j$ , respectively.

$$a_1 = (1 - \tau_1)^{N_1} \quad (5.11)$$

$$a_2 = (1 - \tau_1)^{N_1}(1 - \tau_2)^{N_2} \quad (5.12)$$

$$b_j = 1 - a_j \quad j = 1, 2. \quad (5.13)$$

Then the average frame service time for  $AC_1$  station is given by

$$T_1 = (E[R_1] + E[B_1])(\phi_{1,1}E[S_1] + (\phi_{1,2} + \phi_{2,2})E[S_2]). \quad (5.14)$$

### AC2 stations

The frame service time of a tagged  $AC_2$  station consists of two parts. The first part is the time that the  $AC_2$  station spends in Zone 2,  $T_2^* = (E[R_2] + E[B_2])E[S_2]$ . The other part is called the pre-backoff waiting period as shown in Figure 5.2. This period happens when at least one  $AC_1$  station transmits in Zone 1 and the tagged  $AC_2$  station does not get a chance to decrement its backoff counter at all. The transmission in Zone 1 by at least one  $AC_1$  station can happen consecutively before the tagged  $AC_2$  station decrements its backoff counter, which follows a geometric distribution. The total backoff slots of the tagged  $AC_2$  station can be divided into  $E[B_2](1 - a_2)$  backoff segments. For each backoff segment, there are  $\phi_{1,1}/(\phi_{1,2} + \phi_{2,2})$  pre-backoff waiting periods preceding the actual backoff stage. The newly defined  $\phi_{i,j}$  is introduced by us to solve the excessive overestimation problem in [2].

Following [2], the average length of the pre-backoff waiting periods is given by

$$w = ((1 - a_1) \sum_{i=1}^M a_1^{i-1} ((i - 1)\delta + \Delta)) / (1 - a_1^M). \quad (5.15)$$

Thus, the total time spent in the pre-backoff waiting periods by the tagged  $AC_2$  station is

$$W = E[B_2](1 - a_2)w\phi_{1,1}/(\phi_{1,2} + \phi_{2,2}), \quad (5.16)$$

and the overall frame service time for  $AC_2$  stations is

$$T_2 = T_2^* + W. \quad (5.17)$$

## 5.2 Saturated PCA with DRP

If the inter-arrival time of DRP clusters in a superframe is constant or exponentially distributed with rate  $\omega$ , the expected number of DRP clusters experienced by the tagged  $AC_i$  station is  $D_i = T_i\omega$ . If the length of each DRP cluster is  $\Delta_r$ , the frame service time with the presence of DRP can be estimated by  $\zeta_i = T_i + D_i\Delta_r + D_iAIFS_i + E[R_i]T_Q$ , where  $T_Q$  is the sum of the data frame transmission time, acknowledgment frame transmission time, SIFS and guard time, since as shown in Figure 5.2, the station has to hold on if the remaining time to the next DRP cluster is not sufficient for the entire frame.

## 5.3 Unsaturated PCA without DRP

The difference between the saturated and unsaturated case is that in the former, there is always at least one packet in the transmission queue, whereas in the latter, the queue might be empty from time to time and the achievable throughput is the offered load. Station busy probability is 1 in the saturated case and this is considered as the upper bound, and at this point if more packets come they begin to accumulate in the queue. In our analysis, all symbols for the unsaturated case are superscripted by '. If the frame arrival rates in a random slot of  $AC_1$  and  $AC_2$  stations are  $\lambda_1$  and  $\lambda_2$ , the busy probabilities for  $AC_1$  and  $AC_2$  stations are given by  $\rho_1 = T'_1\lambda_1$  and  $\rho_2 = T'_2\lambda_2$ , respectively. Note that  $T'_1$  and  $T'_2$  are the frame service time for  $AC_1$  and  $AC_2$  stations, respectively.

Therefore we can say in a randomly chosen slot, frame transmission probabilities are  $\tau'_i\rho_i$ ,  $i \in 1, 2$ . Now the collision probability in the case of  $AC_2$  stations is given by just following the previously derived equation



$$P'_2 = 1 - (1 - \rho_1\tau'_1)^{N_1}(1 - \rho_2\tau'_2)^{N_2-1}. \quad (5.18)$$

Similarly for  $AC_1$  stations it is obtained in Zone 1 and Zone 2 respectively

$$P'_{1,1} = 1 - (1 - \rho_1\tau'_1)^{N_1-1}, \quad P'_{1,2} = 1 - (1 - \rho_1\tau'_1)^{N_1-1}(1 - \rho_2\tau'_2)^{N_2}. \quad (5.19)$$

Since the tagged  $AC_1$  station contends with other stations with probability  $\tau'_1$  and other stations contend with the tagged station with probability  $\rho_1\tau'_1$ , the transmission probability of the tagged  $AC_1$  station in Zone 2 is

$$\theta'_2 = (((1 - \rho_1\tau'_1)^{N_1-1})(1 - \tau'_1))^M, \quad (5.20)$$

and the transmission probability in Zone 1 is given by

$$\theta'_1 = 1 - \theta'_2. \quad (5.21)$$

Therefore the average collision probability of the tagged  $AC_1$  station can be obtained by

$$P'_1 = \theta'_1 P'_{1,1} + \theta'_2 P'_{1,2}. \quad (5.22)$$

To get the generic slot length, we need to know the probability of a particular slot being idle and in the unsaturated case, a slot can be idle due to no traffic, which should not be taken into account in frame service time. We assume an  $AC_1$  station tends to transmit in Zone 1, and the probability of a slot being idle in Zone 1 is  $a'_{1,1} = (1 - \tau'_1)(1 - \rho_1\tau'_1)^{N_1-1}$ . If the  $AC_1$  station tends to transmit in Zone 2, the probability of a slot being idle in Zone 2 is  $a'_{1,2} = (1 - \tau'_1)(1 - \rho_1\tau'_1)^{N_1-1}(1 - \rho_2\tau'_2)^{N_2}$ . Therefore,

the generic slot length in Zone 1 and Zone 2 for  $AC_1$  stations can be computed by  $E[S'_{1,1}] = a'_{1,1}\delta + (1 - a'_{1,1})\Delta_1$  and  $E[S'_{1,2}] = a'_{1,2}\delta + (1 - a'_{1,2})\Delta_1$ , respectively.

Similarly, if an  $AC_2$  station tends to transmit in Zone 2, the probability of a slot being idle in Zone 2 due to backoff is  $a'_{2,2} = (1 - \tau'_2)(1 - \rho_1\tau'_1)^{N_1}(1 - \rho_2\tau'_2)^{N_2-1}$ . The generic slot computation for  $AC_2$  is the same as  $AC_1$  in Zone 2, which is given by  $E[S'_{2,2}] = a'_{2,2}\delta + (1 - a'_{2,2})\Delta_2$ .

The frame service time for  $AC_1$  stations and the first part of the frame service time for  $AC_2$  stations can be derived in the same way as that in the saturated case.

To calculate the pre-backoff waiting period per backoff segment of  $AC_2$  stations, we have to solve following equations

$$\phi'_{1,1}/\phi'_{1,2} = \theta'_{1,1}/\theta'_{1,2} \quad (5.23)$$

$$(\phi'_{1,1} + \phi'_{1,2})/\phi'_{2,2} = \rho_1\tau'_1/(\rho_2\tau'_2) \quad (5.24)$$

$$\phi'_{1,1} + \phi'_{1,2} + \phi'_{2,2} = 1 \quad (5.25)$$

The definition of  $\phi'_{i,j}$  is the same as that in the saturated case, which is introduced by us to solve the overestimation problem. The pre-backoff waiting period for  $AC_2$  stations is derived in a similar way as that in the saturated case, so is the frame service time for  $AC_2$  stations.

Then with the two more inputs  $\lambda_1$  and  $\lambda_2$ , we need to solve six equations to get the value of unknown variables  $\tau'_1$ ,  $\tau'_2$ ,  $P'_1$ ,  $P'_2$ ,  $\rho_1$ , and  $\rho_2$ . Finally with the values of  $\lambda_1$ ,  $\lambda_2$ ,  $\rho_1$  and  $\rho_2$ , we get the unsaturated frame service time for both classes.

## Chapter 6

# Video Streaming over UWB

## Wireless Networks Simulation

In this chapter, we evaluate the performance of video streaming over UWB wireless networks through the analytical calculation and the network simulation. Since video traffic is quite bursty and it is difficult to capture the behaviour of video traffic analytically, we validate our model in terms of frame service time with simulation considering that the traffic arrival rate follows Poisson distribution. Through validating the model with Poisson traffic, we can get the performance bound of the video traffic. Afterwards, we focus on the video streaming performance evaluation through simulation and considering WiMedia UWB MAC specific parameters: hard DRP, soft DRP, TXOP etc. After observing all results we determine the admission region or maximum capacity of the network.

## 6.1 Model Validation

### 6.1.1 Simulation Methodology

To verify the accuracy of the analytical models, we have done extensive simulation in *NS-2*. Since *NS-2* does not have the module for WiMedia UWB MAC layer and the PCA is similar to IEEE 802.11e, we have modified TKN's EDCA code [17] to simulate the behavior of WiMedia UWB MAC. We have also modified the IEEE 802.11 physical layer module in *NS-2* to emulate the MB-OFDM UWB physical layer. We used the free-space propagation model with ideal channel condition in simulation. Therefore packet loss in the MAC layer happens only due to collision among multiple packets. Propagation delay is assumed as zero and in order to obtain this we have set the propagation time in simulation as zero. All the parameters we have used for validation are listed in Table 6.1. We assume the number of  $AC_1$  and  $AC_2$  stations is the same, i.e.,  $N_1 = N_2$ . Network is like a piconet where all nodes can hear each other, which has been shown in Figure 6.1. All the stations on the circumference of the circle transmit packets to the base station in the centre of circle. The role of the base station is just to receive packets from all transmitting stations. In order to avoid the routing packets of the ad-hoc routing protocol provided by the *NS-2* wireless simulation module, we adopted the *NOAH* [25] extension for static routing scheme for our specific topology to get the correct packet delivery path. The frame arrival events at each station follow a Poisson process.

### 6.1.2 Validation of PCA Performance without DRP

Figure 6.2 shows the frame service time affected by the increased frame arrival rate. The number of contending stations in this scenario is  $N_1 = N_2 = 9$ . When the frame arrival rate is low, the channel becomes idle from time to time due to no traffic.

Table 6.1: Parameters Used for Performance Evaluation

Data Rate	480 Mbps
$AIFSN_1$	2
$AIFSN_2$	4
$minCW_1$	8
$minCW_2$	15
Slot Time ( $\delta$ )	9 us
SIFS	10 us
Guard Time	12 us
Frame Payload	1024 Bytes
Retry Limit	7

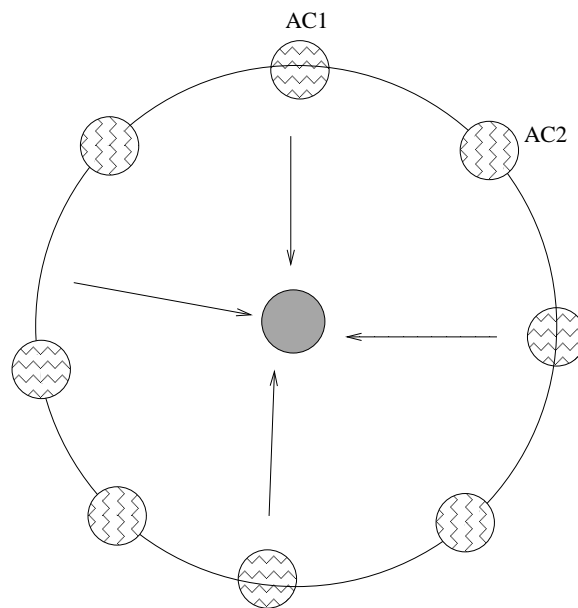


Figure 6.1: Network Topology

Therefore, there is a low chance to have collisions with other frames from other stations, and thus the frame service time is pretty low (i.e., dominated by frame transmission time) for both  $AC_1$  and  $AC_2$  stations.

As the offered load is increased, we observe an increased frame service time due to the increased number of collisions. The increased offered load affects the low priority traffic more than the high priority traffic. This is because as the offered load is increased, there is a higher chance that  $AC_1$  stations have frames to transmit, which in turn increases the probability that at least one  $AC_1$  station transmits in Zone 1. This scenario increases the likelihood of pre-backoff waiting periods for  $AC_2$  stations and ultimately their frame service time. Due to the increased frame service time, with the same offered load  $AC_2$  stations become saturated earlier than  $AC_1$  stations, as being pointed out in the figure. After  $AC_2$  stations are saturated, with the increased offered load and more collisions, the frame service time for  $AC_1$  stations is increased as well but much slower when compared with  $AC_2$  stations. If we further increase the offered load,  $AC_1$  stations get saturated eventually as well. At this point we see the maximum frame service time for both classes of stations, beyond which they will experience excessive queuing delay. This figure also shows that our improved analytical models provide a much tighter upper bound than the ones in [2], especially for  $AC_2$  stations, in both unsaturated and saturated cases.

Figure 6.4 shows that simulation results are in good agreement with the analytical ones as the total number of stations ( $N_1 + N_2$ ) is increased when the offered load is 0.004 frames/slot/station. As the number of stations increases, frame service time increases as well since the larger the number of stations the larger the number of collisions, and eventually it results in an increased frame service time. This figure illustrates again that low priority stations are more affected in terms of the increased frame service time than high priority ones. This is because as the number of  $AC_1$

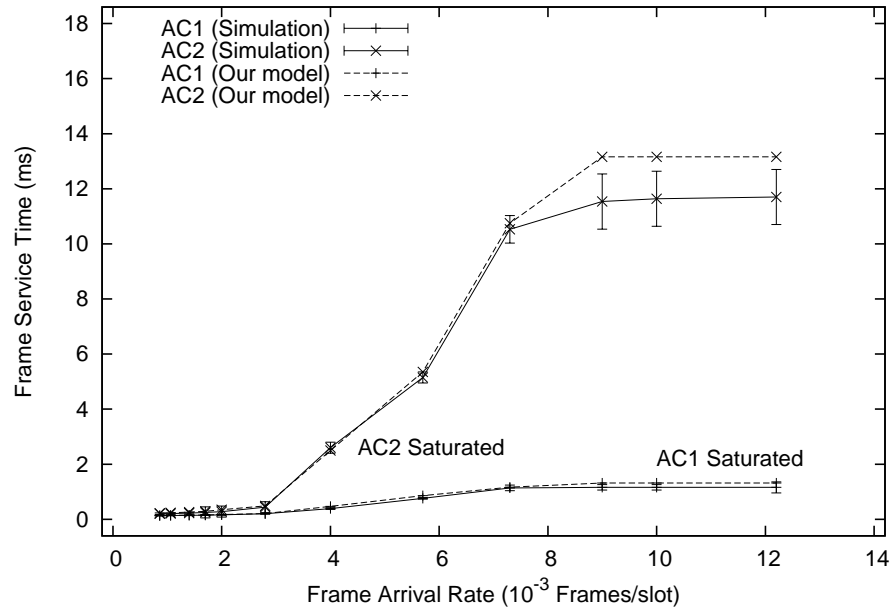


Figure 6.2: Average Per Station Frame Service Time vs. Frame Arrival Rate

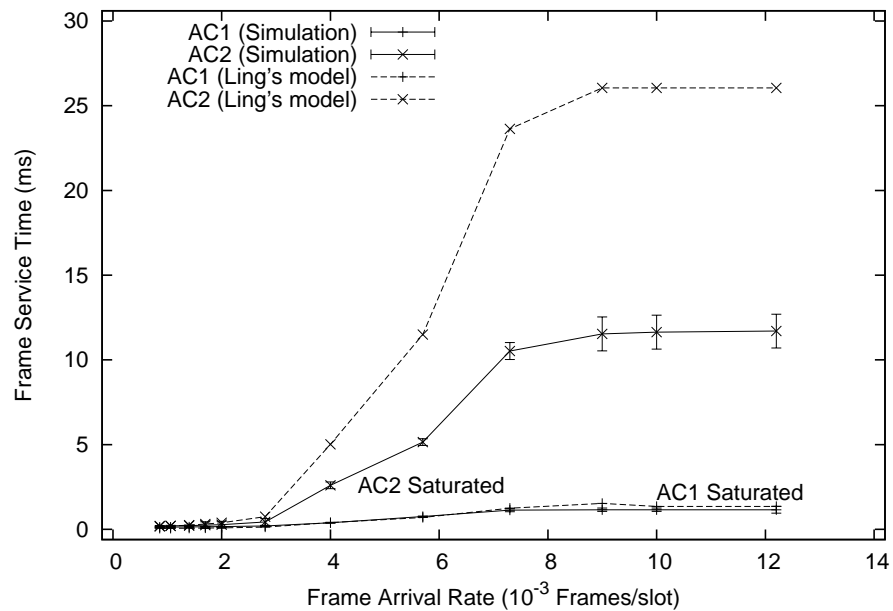


Figure 6.3: Average Per Station Frame Service Time vs. Frame Arrival Rate

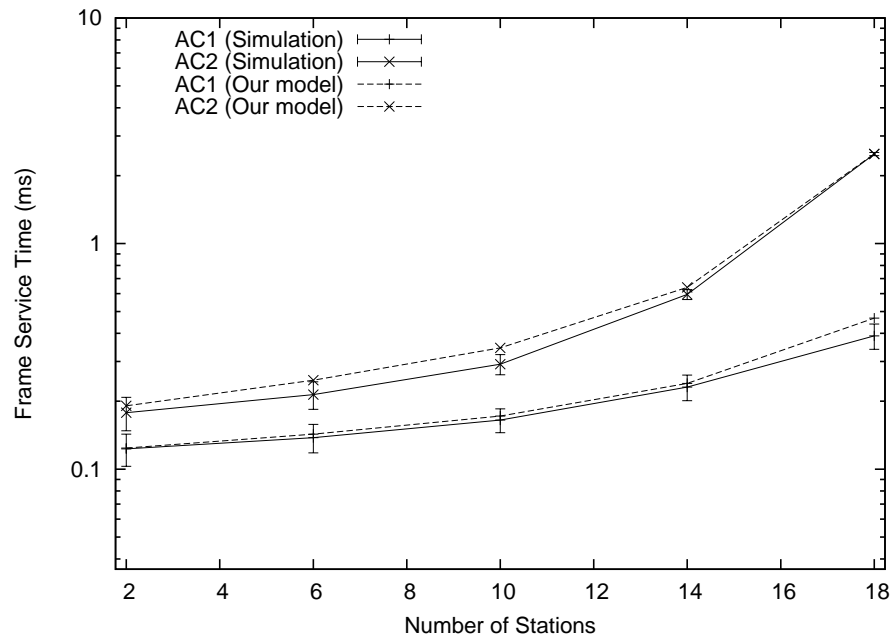


Figure 6.4: Average Per Station Frame Service Time vs. The Number of Stations

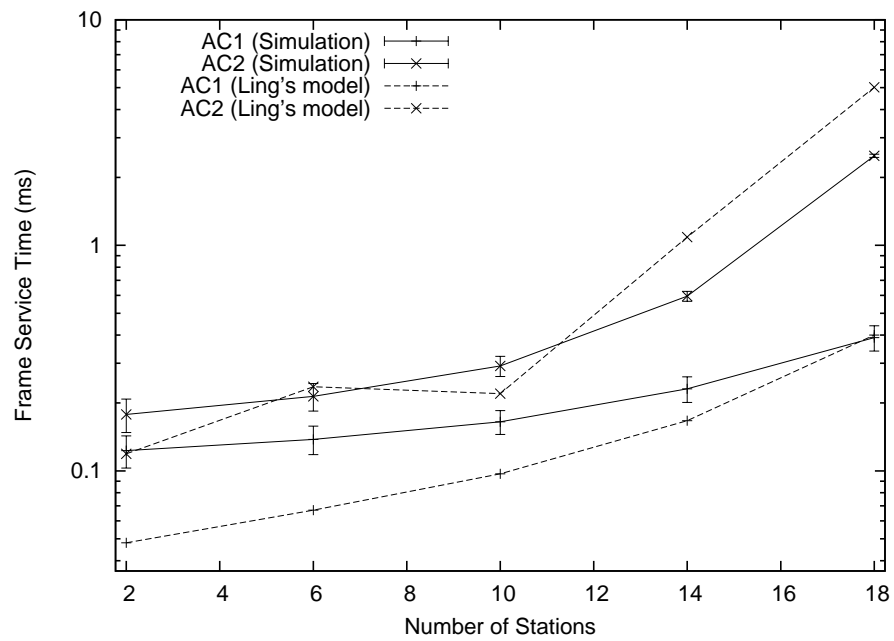


Figure 6.5: Average Per Station Frame Service Time vs. The Number of Stations



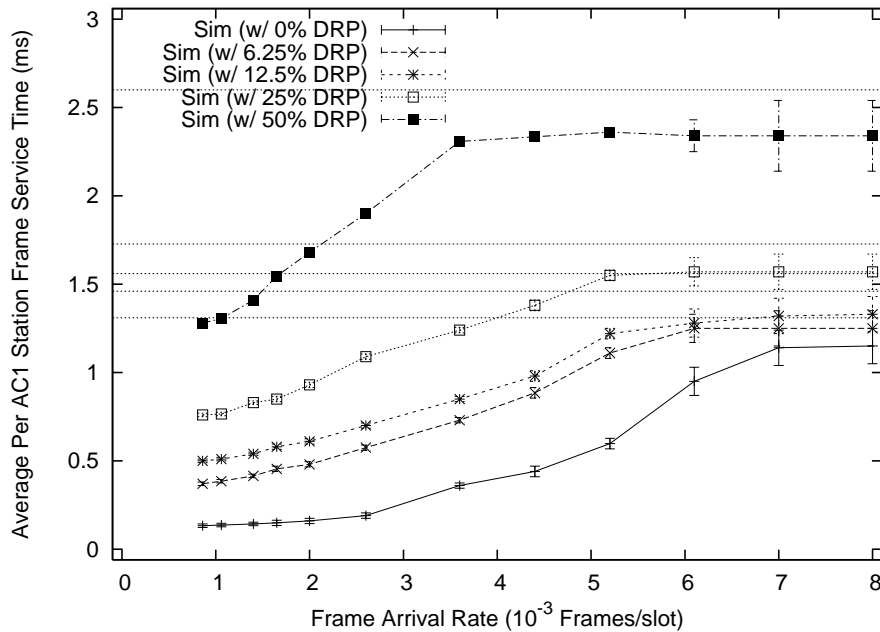


Figure 6.6: Average Per AC1 Station Frame Service Time vs. Frame Arrival Rate

stations is increased, the probability that at least one  $AC_1$  station transmits in Zone 1 also increases, which causes again an increased likelihood of pre-backoff waiting periods for  $AC_2$  stations and ultimately their frame service time. This figure also shows our models give better prediction than [2], even at a very low load.

### 6.1.3 Validation of PCA Performance with DRP

In order to see the effect of DRP on PCA frame service time, we put some hard DRPs in a superframe with different DRP reservation percentage: 12.5%, 25% and 50%. These DRPs are distributed as even as possible across the superframe. The frame transmission over DRP is deterministic and the delay is guaranteed. Except the portion reserved for DRP, the rest of the DTP in the superframe is available for PCA. In our simulation, during DRP periods all PCA stations keep silent, and after the DRP periods, they start their usual activities again (backoff, transmission, etc).

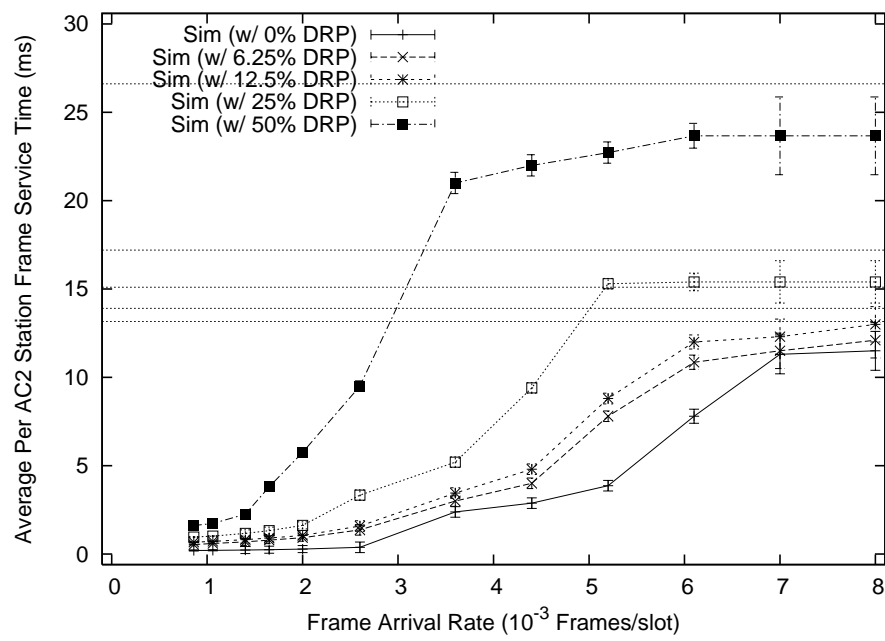


Figure 6.7: Average Per AC2 Station Frame Service Time vs. Frame Arrival Rate

The number of PCA stations for this scenario is also  $N_1 = N_2 = 9$ .

The results in Fig. 6.6 and Fig. 6.7 compare the frame service time with the presence of DRP at different percentage for  $AC_1$  and  $AC_2$  stations, respectively. In these two figures we gradually increase the frame arrival rate and plot the corresponding frame service time. When there are more DRP clusters, the PCA frame service time is increased accordingly since there is less time available for PCA and therefore it takes a longer time to have a successful frame transmission. These figures again point out that at the same offered load,  $AC_2$  stations with a higher percentage of DRP get saturated much earlier. Due to the increased number of pre-backoff waiting periods caused by the increased offered load and resultant increased number of collisions, as well as less available PCA time. If the percentage of DRP is  $X$  and if the frame service time is  $T$  when the whole DTP is available for PCA, at the system saturated point (when both classes of stations get saturated), the frame service time with the presence of DRP is approximately  $T/(1 - X)$ , which has been reflected in these figures as well. Saturated service time with the presence of DRP, shown in dotted lines, also matches the numerical results from our analysis. At a very low offered load, the frame service time with the presence of DRP mainly depends on DRP cluster length. This is because at a very low load the frame service time without DRP is usually pretty low, and occasionally if any frame transmission is postponed by a DRP cluster, the length of that DRP cluster dominates the overall PCA frame service time.

#### 6.1.4 PCA performance and TXOP

One of the MAC layer features of UWB wireless networks is TXOP. Due to this property of the MAC layer, once any station gets the channel when the backoff counter is zero it can transmit multiple frames back to back separated by SIFS time depending on the TXOP parameter. If any packet is collided in TXOP duration, the station

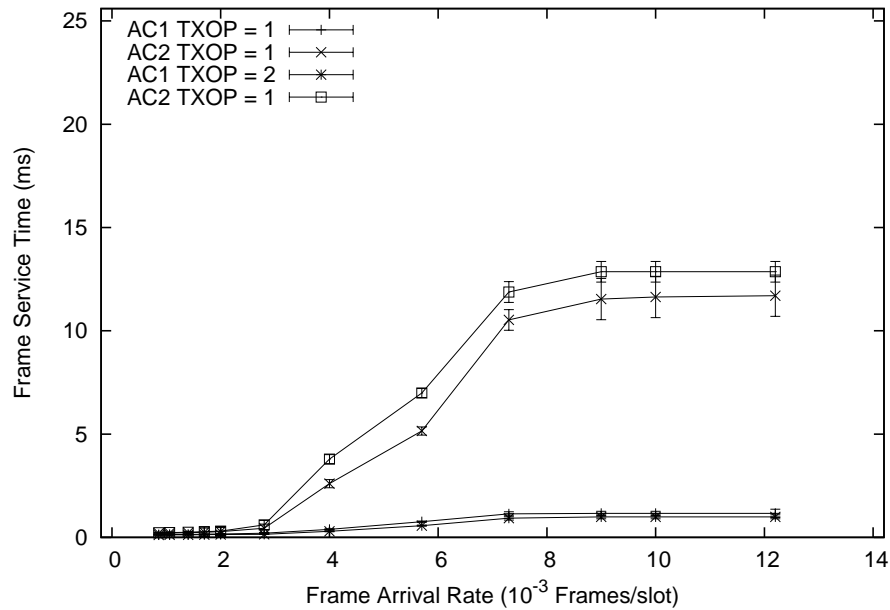


Figure 6.8: Average Per Station Frame Service Time vs. Frame Arrival Rate

transmitting that packet goes to the backoff stage again and retransmits the packet when the backoff procedure is finished. Figure 6.8 shows that the frame service time of  $AC_1$  station is lower when the TXOP duration is bigger with the increasing packet arrival rate. As the TXOP gets smaller the frame service time for that case is larger. Since  $AC_1$  holds the channel longer for a larger TXOP,  $AC_2$  station gets less chance to access the channel and thus the frame service time is also increased. Another observation is that  $AC_2$  station gets saturated earlier with the increased TXOP duration of  $AC_1$  station. In this scenario we have kept the TXOP duration of  $AC_2$  station fixed at 1 packet. In addition in this figure we have not shown any analysis results. Again the total number of stations in this case is 18.

## 6.2 Performance Evaluation of Video Streaming over UWB Wireless Networks

In this section, we evaluate the performance of video streaming over UWB wireless networks by *NS-2* simulation. Video flows, particularly those compressed by H.264 encoders, have high burstiness and generate Variable Bit Rate (VBR) traffic. Video streaming is very sensitive to packet loss which ultimately causes frame loss. In addition to frame/packet loss, video streaming is also sensitive to network delay and jitter. Therefore, in this section, we focus on PSNR, an objective video quality metric, and frame delay and jitter for video streaming performance evaluation. We send the video over PCA, PCA with hard DRP and then PCA with soft DRP, and see how the performance of video streaming is affected in terms of frame service time, packet loss, frame loss, delay, jitter etc.

### 6.2.1 Soft and Hard DRP Implementation

According to the WiMedia UWB MAC specification [1] DRP has two variations: one is soft DRP and another one is hard DRP. As we mentioned previously that in the DRP period, station or node gets exclusive access of the channel. When it is soft DRP, if the DRP owner station does not have any packet to transmit, it can give the DRP period to other stations to use as just a PCA period. Whereas if it is hard DRP and during the DRP period even if the DRP owner does not have any packet to transmit, other stations cannot access the channel during this period. Therefore intuitively we can say that through soft DRP, channel utilization is better than that with hard DRP. We put some DRPs (soft/hard) across the super frame as uniformly as possible and all stations in the network own the equal number of DRP slots. During DRP period, to transmit a packet the tagged station first goes to the AIFS period corresponding

to the AIFSN length as 1 and then zero backoff slot before transmitting the data packet.

### 6.2.2 Methodology

For the video streaming simulation, we have used the almost same general procedure as we have discussed in the model validation section. However for the simulation scenario, we have only used  $AC_1$  traffic. To produce the video streams in the simulation, we have used the contributed code from *EvalVid* [22]. This code has a bunch of programs to generate video trace and generate trace files in simulation. Later on we have used *EvalVid* [22] to analyze these trace files and get all quality metrics.

In the experiment, we have used H.264 encoded 4 HDTV demo video clips with data rate 4.86 Mbps which emulates a typical quad HDTV video file. In simulation we have used one MPEG4 AVC encoded video file instead of 4 video files with data rate 5.03 Mbps. Peak rate of this video file is 51.9 Mbps. The maximum and average frame size of this video are 270,744 and 1,004 bytes, respectively. The video streaming traffic uses UDP/RTP as the transport layer protocol. The overhead of IP, UDP and RTP are 20, 8 and 12 bytes, respectively. All the performance results are the average of 9 runs from simulation.

We evaluate the video streaming performance with multiple concurrent video streams considering as  $AC_1$  traffic. There is no  $AC_2$  traffic in the network even though we validate our model in terms of frame service time considering there are both  $AC_1$  and  $AC_2$  traffic in the piconet. In order to investigate the maximum capacity of the UWB wireless networks with data rate 480 Mbps, up to 14 video streams were evaluated. From the simulation, we find that the video quality of each single stream in multiple streams is statistically equivalent. Therefore, we only present the results of the first video stream of the multiple streams in the following sections. We

compare the video streaming performance when the whole time period is for PCA, then with some hard DRPs interleaved with PCA and then with some soft DRPs. From our observation of the simulation results we have found that video performance is the best when we put some soft DRP in the supreframe interleaved with PCA. In this case actually more than 14 video streams (around 15) can be supported in the network with satisfactory QoS requirement when the number of reserved DRP slots is less. Video streaming performance over PCA with hard DRPs is the worst and with hard DRP barely 12 video streams can sustain in the network. 10 video streams can fairly be transmitted with the PSNR of received reconstructed video in the acceptable range. And therefore for the purpose of comparison between the performance of soft DRP and hard DRP, we have assumed there are 10 video streams in the network. Knowing that soft DRP performance is the best we have found the admission region or the maximum capacity of the network with soft DRP and hard DRP in the later subsection.

### 6.2.3 Collision Probability & Frame Service Time

Figure 6.9 and Figure 6.11 show how the collision probability and the frame service time are affected by the increasing number of DRP slots per station. We see different trends for the soft DRP and hard DRP scenarios. In these figures when the number of DRP slots is zero, it implies the PCA only case. According to the soft DRP results, as the number of reserved slots is increased, collision probability and frame service time are almost in steady state when number of video streams is 10. Since the number of stations in this case is low, the total number of DRP slots is less with respect to the total number of DRP slots in the superframe. A small number of DRP slots means less interruption of PCA slots and therefore less overhead due to backoff and collisions. During DRP slot owner station's packet can be transmitted

with very low overhead. Again due to the property of soft DRP, if there is no traffic in owner station's DRP slot, that slot can be used as PCA slot for other stations. These extra advantages of soft DRP are balanced with the overheads introduced by the interruption of PCA slots when other stations' DRP comes. Therefore the overall collision probability and frame service time remain in the certain range even though due to randomness there is a bit fluctuation. However when the number video streams is increased, the collision probability and the frame service time are decreased first and then increased with the increasing number of reserved DRP slots. This is because, a small number of reserved slots can be efficiently utilized and the number of packets left for contention in PCA is greatly reduced. With less contention, the overhead (collisions and backoff) in PCA periods can be reduced as well. When the number of reserved slots is large, since the duration of a MAS slot for DRP ( $256 \mu\text{s}$ ) is much longer than that of a fixed contention slot for PCA ( $9 \mu\text{s}$ ), frequent interruption by DRP brings up the service time in PCA. In addition, with a large number of reserved DRP slots, the DRP slots are not efficiently utilized, but the remaining channel time for PCA is significantly reduced, which results in a higher contention level and the higher collision probability and the longer service time. The collision probability and frame service time "bounce-back" behavior introduces a tradeoff between the number of MAS slots reserved for each video flow and the total number of video flows. We will investigate this tradeoff and find the maximum capacity of the network in the later subsection. Whereas in the hard DRP case, we see as the number of reserved slots is increased the collision probability and frame service time are increased gradually. This increasing behavior is not very sharp at the beginning, however as the number of reserved slots is increased, the collision probability and frame service time increase abruptly. As we mentioned, in the case of hard DRP a reserved slot cannot be used for PCA even though the reserved slot is not used. When the number of reserved



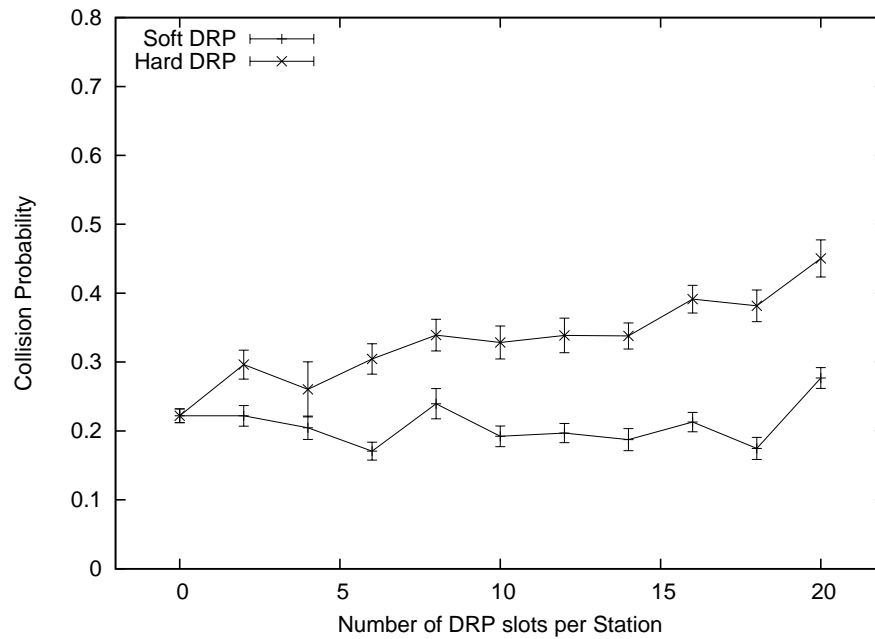


Figure 6.9: Collision Probability vs. The Number of DRP slots per station

slots is less, slots are used efficiently and therefore frame service time is not increased that much, however as the number increases many slots become idle due to no traffic and the PCA period available for video transmission becomes less and due to PCA's overhead the frame service time increases considerably.

Figure 6.10 and Figure 6.12 show how the number of video streams affects the collision probability and frame service time when the number of reserved MAS slots is 10. It is intuitive that as the number of stations is increased there will be more traffic. More traffic means more stations try to access the channel and therefore more collisions. Again more collisions indicate more backoff slots and transmission slots and finally the increased frame service time.

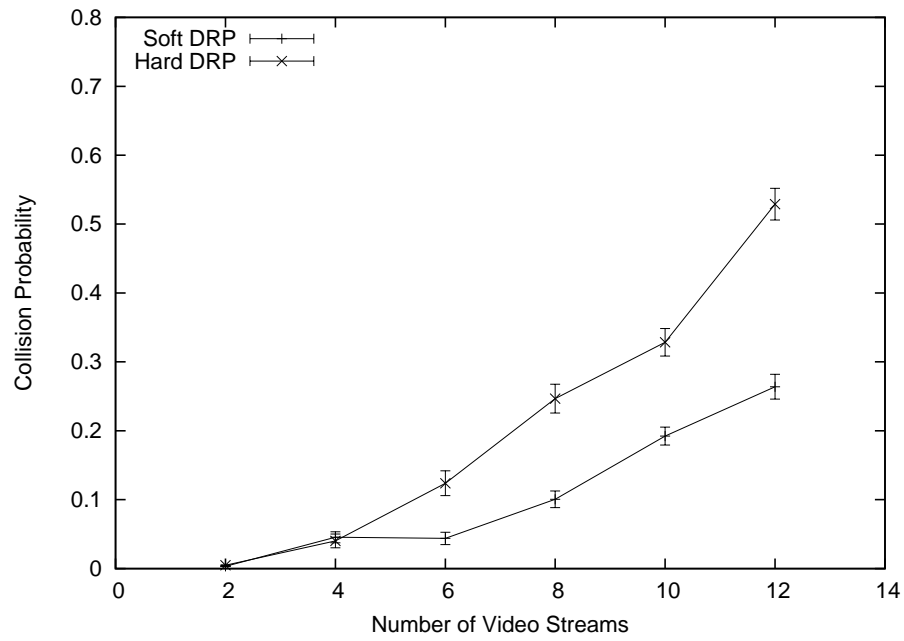


Figure 6.10: Collision Probability vs. The Number of Video Streams

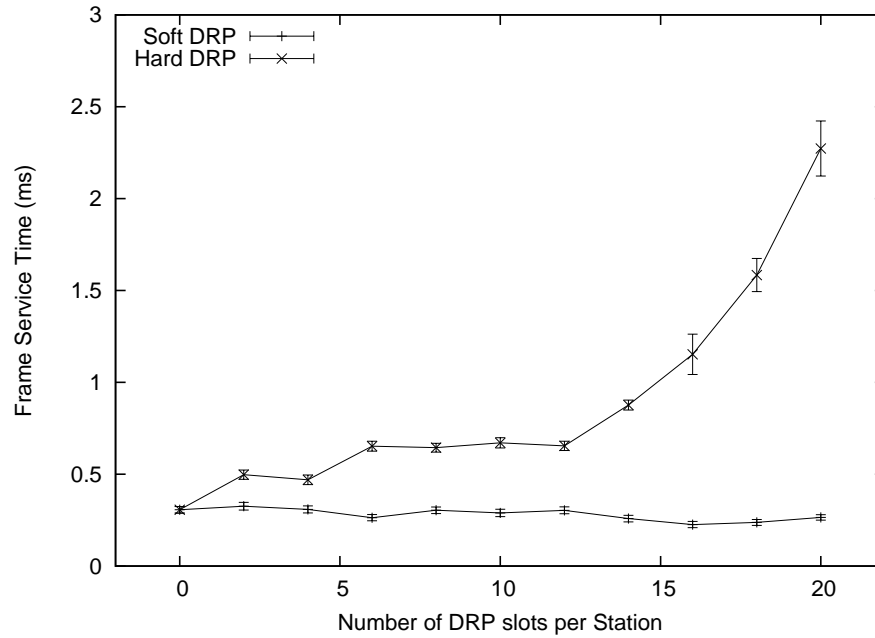


Figure 6.11: Average Per Station Frame Service Time vs. The Number of DRP slots per station

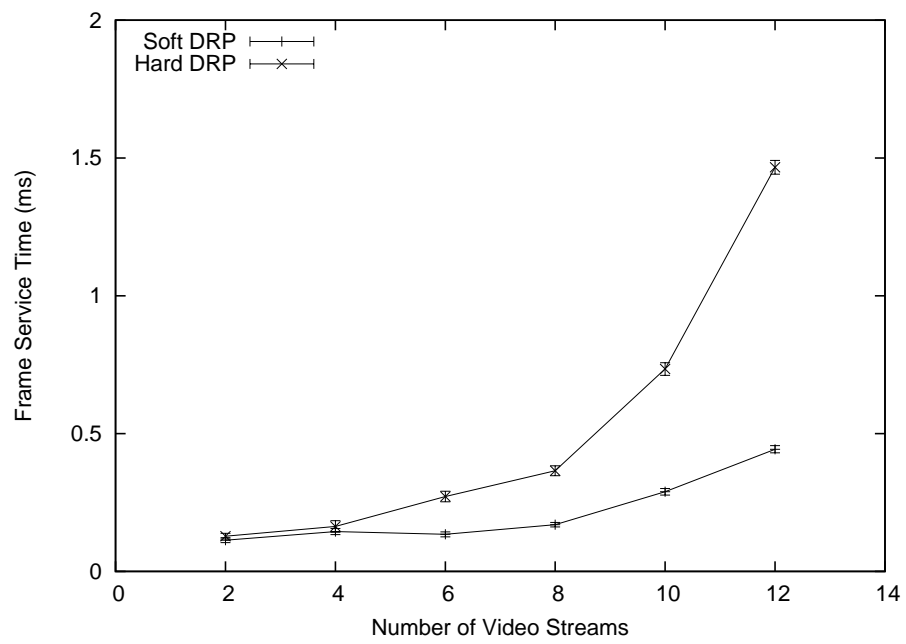


Figure 6.12: Average Per Station Frame Service Time vs. The Number of Video Streams

### 6.2.4 Packet Loss

Figure 6.13 shows the I-frame packet loss ratio ( $PLR_I$ ) of the video stream with the PCA, the PCA with soft DRP and the PCA with hard DRP. I-frame is the most important in all three types of frames since the decoder uses the content of I-frame to decode other frames in the same GOP. If the content is lost in the I-frame, the error is propagated to all the other frames in the same GOP. Packet loss in a P-frame or B-frame only affects a few neighbour pictures or just itself, and the impact of this loss on the video quality can be minimized by the H.264 error concealment algorithm. Therefore, the  $PLR_I$  is an important metric for video quality. According to [3], when  $PLR_I$  is above 5%, the PSNR of the received video is usually less than 36 dB, and the perceptual quality is poor. As we see the results in the previous subsection that the video streaming performance of the soft DRP case is the best in terms of the collision probability and frame service time. The same thing is observed in this scenario. The PLR is decreasing at the beginning when the number of reserved slots is small and then increased with the increasing number of reserved slots. However according to the figure, when the number of video streams is 10, the PLR of I frame is quite in a certain stable range in the case of the soft DRP scenario. This is again due to the reason we mentioned in the Collision Probability & Frame Service Time subsection. With the increased number of video streams, as the number of reserved slots is increased, collision probability is increased and due to the high collision probability it is more likely that the number of retransmissions for each packet exceeds the retry limit. This leads to packet drop in the MAC layer and increases the PLR as well. As the number of DRP slots is increased, the slots for the PCA period are decreased gradually, however due to the high burstiness of H.264 encoded video, the traffic needs to be transmitted overweighs the time available for the PCA period and therefore there is packet loss due to interface buffer overflow. Due to the difference between soft DRP

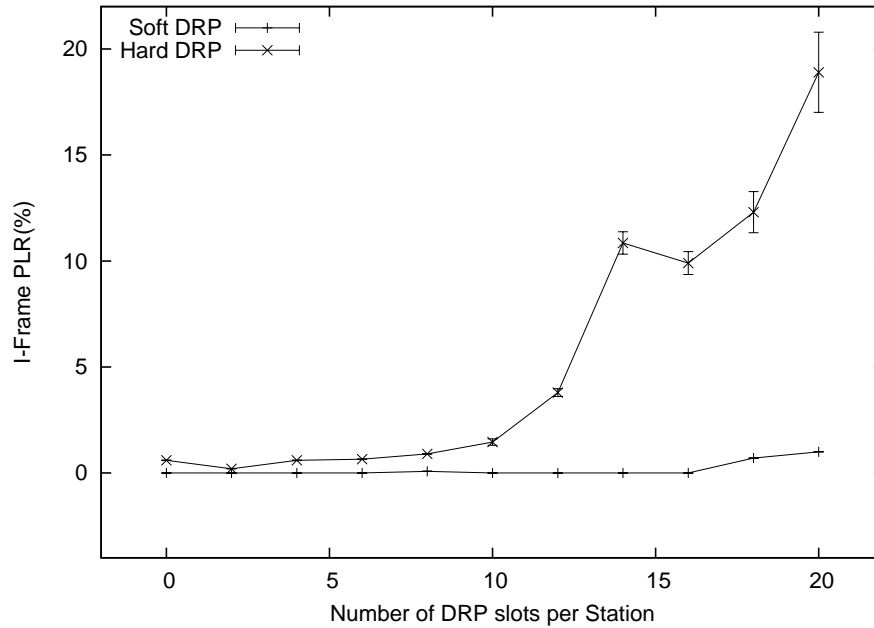


Figure 6.13: I-Frame PLR (%) vs. The Number of DRP slots per station

and hard DRP, packet loss is harsher in the case of hard DRP.

According to the Figure 6.14, we observe the percentage of I-frame packet loss is increased with the increasing number of video flows given that the number of reserved DRP slots per station is 10. When the number of video streams is very few, I-frame packet loss is almost 0 even though there might be some packet loss in P-frame and B-frame. Again due to the nature of the hard DRP, the percentage of packet loss is worse for this scenario.

### 6.2.5 PSNR

As an objective video quality metric, PSNR is the fidelity indicator of the reconstructed received video. A higher PSNR indicates that the received video has a higher quality. Figure 6.15 shows the average PSNR of the target video stream for the soft and hard DRP scenario with the increasing number of reserved slots. PSNR

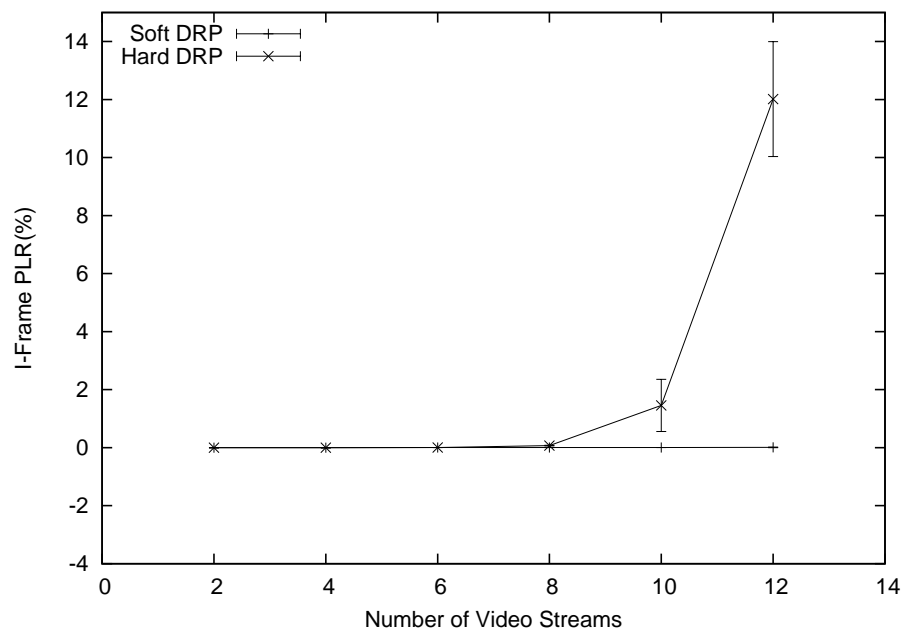


Figure 6.14: I-Frame PLR (%) vs. The Number of Video Streams

depends on the packet loss especially the packets of I-frame. *EvalVid* tries to recover the packet loss in other frames, however if the packet loss in I-frame is greater than 5%, video quality is not in the acceptable range. The maximum number of video streams supported in the case of soft DRP is more than 14 with the acceptable video quality range. In fact, 15 video streams can be allowed in the network when the number of reserved DRP slots is less. Beyond the number of video streams 15, with the large number of DRP reserved slots due to the higher I-frame PLR, the PSNR gets degraded. With the PCA only case the maximum number of supported video streams is 12 with little lower video quality. Since with hard DRP, the performance becomes worse with the increasing number of reserved DRP slots, the maximum number of video streams can be supported with hard DRP is less than 12 when the number of reserved slots per station is very few.

As shown in Figure 6.16, the average PSNR decreases when the number of concurrent video streams increases, because the increased contention for wireless channel due to more traffic results packet drop due to exceeding the number of transmission attempts beyond the retry limit. Again the high burstiness of H.264 encoded video stream easily causes interface buffer overflow with the increased number of video streams.

### **6.2.6 Frame Jitter**

In addition, frame jitter is also a very important metric for video streaming. Frame jitter is defined as the difference between receiver side inter-frame and sender side inter-frame gap. Maximum accumulated jitter is the summation of all jitters from the first frame to the current frame. The maximum accumulated frame jitter determines the minimum initial buffering time and buffer size required to support video streaming without running into buffer outage. In general, a lower frame delay and jitter leads to

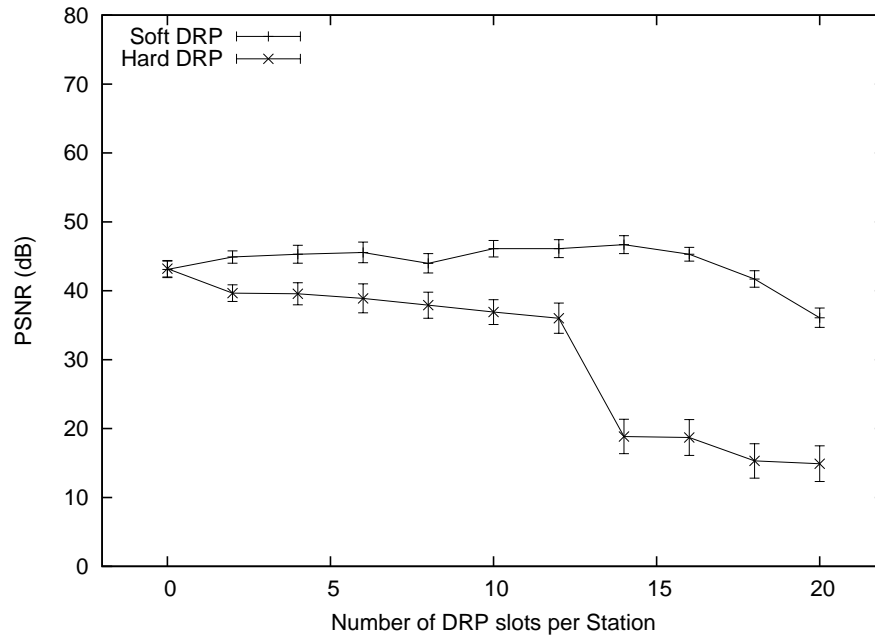


Figure 6.15: Average PSNR (dB) vs. The Number of DRP slots per station

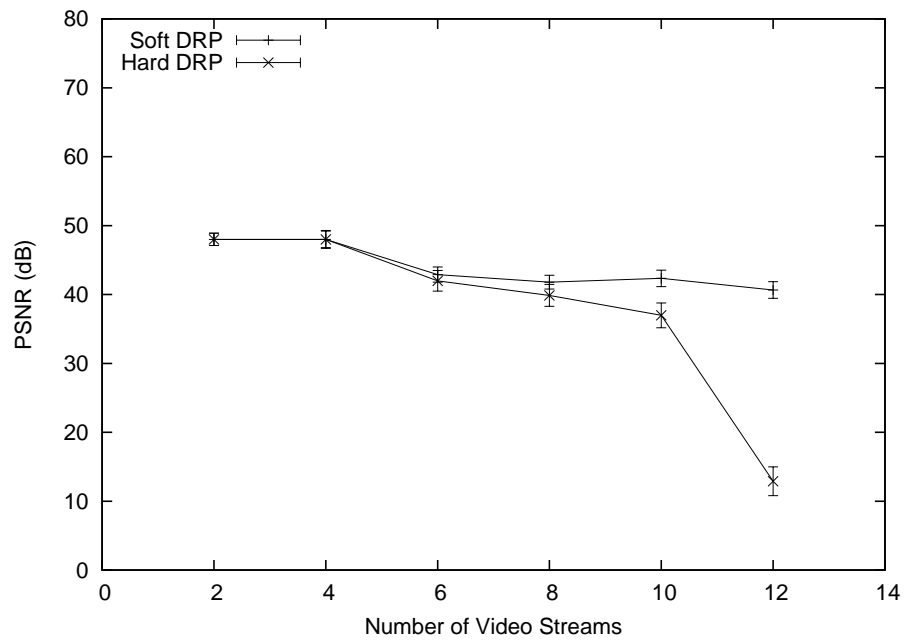


Figure 6.16: Average PSNR (dB) vs. The Number of Video Streams



a better video streaming experience. Figure 6.17 shows the maximum accumulated frame jitter of the first video stream that is mixed with other concurrent video streams. Again the performance of the soft DRP is better compared with PCA only or PCA with hard DRP cases. Due to the lower service time of the soft DRP, the variation of service time is lower and therefore it results in a lower maximum accumulated jitter which has been reflected in the figure pretty well. According to the figure, the maximum accumulated jitter is in a certain range even though there is little fluctuation. For the hard DRP, as the number of the reserved slots is increased the variation of frame service time is increased and therefore the increased jitter which leads to a higher maximum accumulated jitter. As observed in the figure, when the number of DRP reserved slots is 8, we see a big fluctuation of maximum accumulated jitter than the usual trend and this is due to the randomness. In addition when the PLR gets higher with the increased number of reserved slots (more than 12 reserved slots per station), the maximum frame jitter does not increase any further. Since the jitter of lost packets cannot be counted, when the packet loss ratio is high, the maximum accumulated jitter tends to be saturated. Therefore, the jitter data is more meaningful when the packet loss ratio is at a low level.

Figure 6.18 indicates that as the number of video streams is increased, maximum accumulated jitter is increased. The more the number of video flows the higher the frame service time which leads to the higher variation of service time and the higher maximum accumulated jitter as well. However for the hard DRP case, when the number of video streams is 12 due to the considerable amount of I-frame PLR, maximum jitter is not meaningful at this data point.

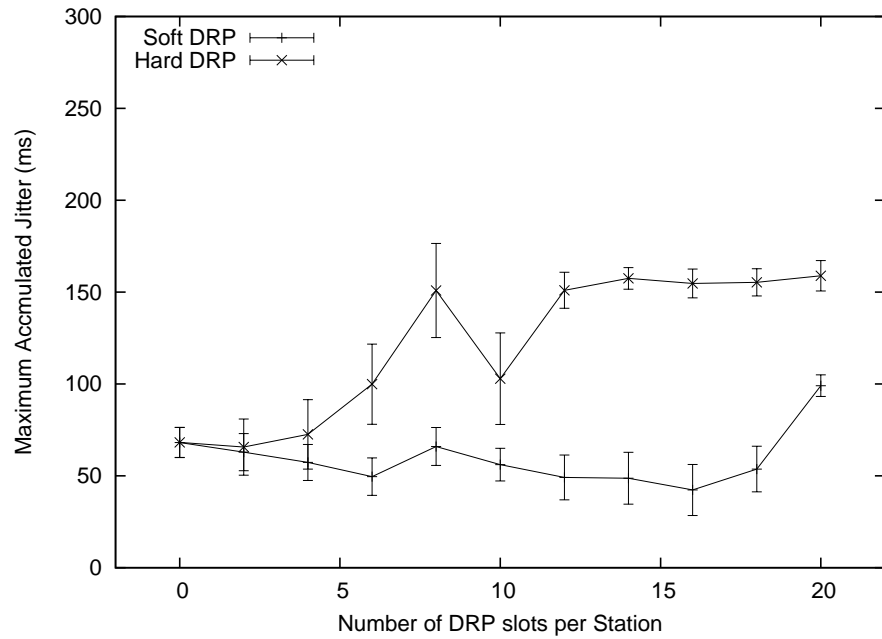


Figure 6.17: Maximum Accumulated Jitter (ms) vs. The Number of DRP slots per station

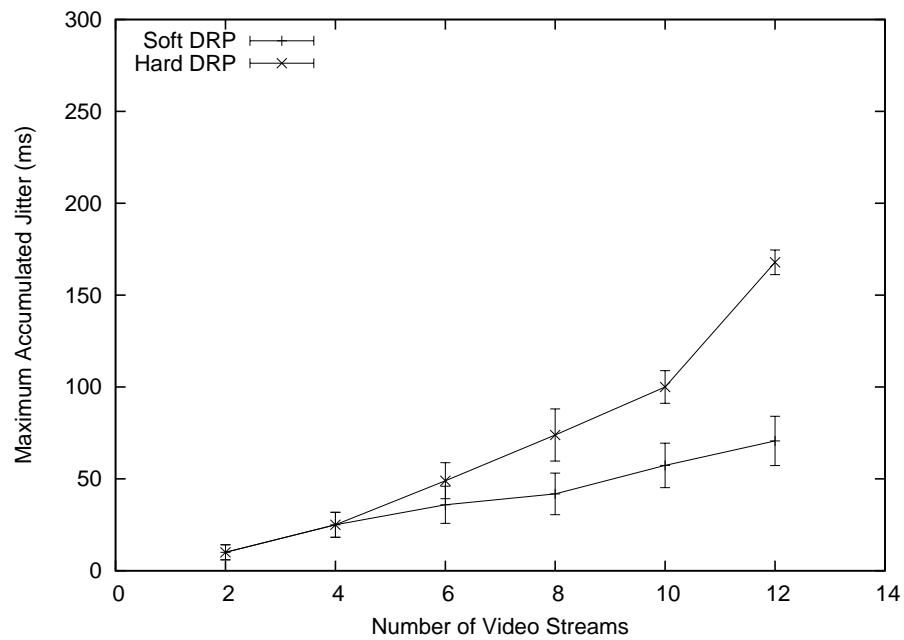


Figure 6.18: Maximum Accumulated Jitter (ms) vs. The Number of Video Streams

### 6.2.7 Admission Region

The admission region is determined by ensuring both PSNR and delay jitter for video streams to meet their QoS requirement. For IPTV-like applications, PSNR should be more than 36 dB and the delay jitter should be less than 100 ms. Both of these parameters have been determined and we have shown the performance the results under different scenarios.

According to our simulation results, the maximum number of video streams can be supported with the PCA only case is around 12 with satisfactory quality of service requirement in terms of both PSNR and the maximum accumulated jitter. Whereas in the hard and soft DRP cases, this number becomes less than 12 and more than 14 respectively. In fact soft DRP can support more than 14 video streams when the number of reserved slots per station is low. Therefore, we can conclude that soft DRP is the best solution for UWB wireless networks and this is new the feature of UWB MAC. However if we want to support more video streams even with soft DRP we need to strike a balance between the number of reserved slots and the number of video streams according the simulation results described above.

## 6.3 Summary

In this chapter, we have investigated the performance of H.264-based video streaming over UWB wireless networks by network simulation. In order to simulate UWB MAC with all its new features we have modified TKN's implementation of EDCA code to get the behaviour of UWB MAC. We also have developed a dummy MBOA UWB physical layer in *NS-2*. Extensive simulations have been done on the video streaming over UWB wireless networks.

In our experiment, due to the limitation of commercially available products we

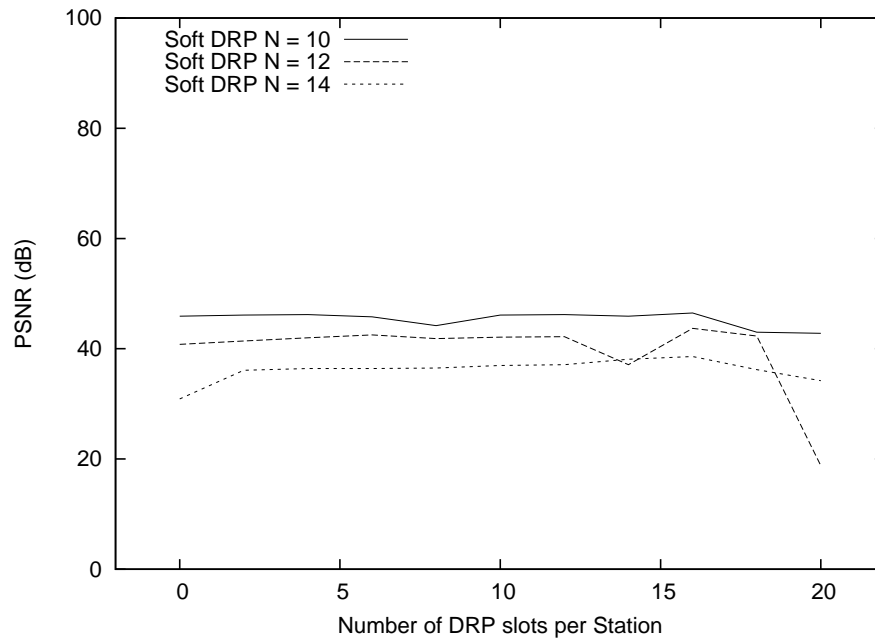


Figure 6.19: Admission Region With Soft DRP

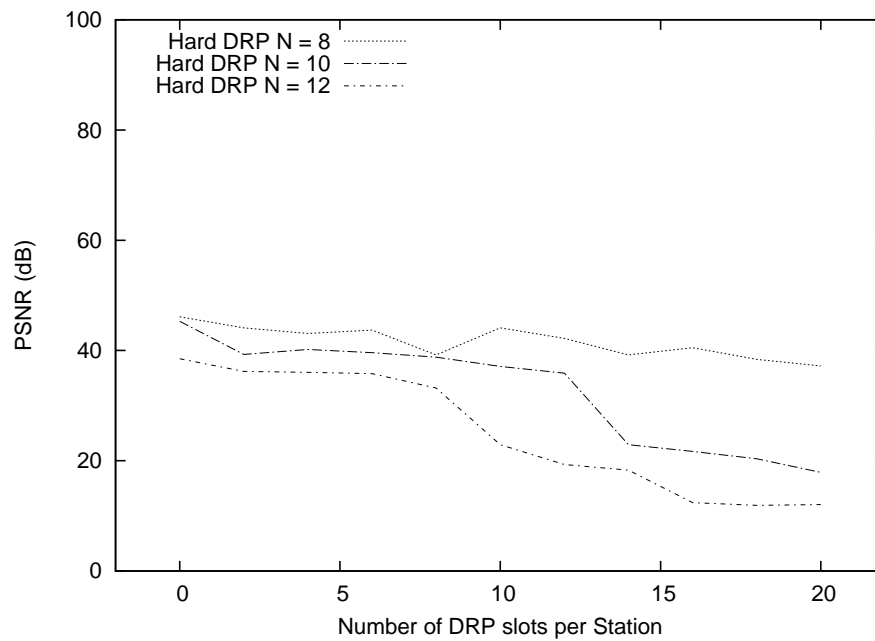


Figure 6.20: Admission Region With Hard DRP

could not study the performance of PCA protocol. In addition to the development of important UWB MAC layer modules we have incorporated some distinct features of UWB MAC, such as soft DRP, hard DRP, TXOP in the module. We have validated our analytical model of the PCA performance with the simulation. Since the only DRP performance in terms of delay or throughput is deterministic, we only have shown the simulation results for the PCA only, the PCA with soft DRP and then the PCA with hard DRP cases. From our observation of simulation results, we have found that the soft DRP performance is the best in terms of the maximum number video streams with satisfactory QoS requirement. However one tradeoff we have obtained is the number of reserved DRP slots and the number of video streams. When the number of video flows is less than 12, video stream's quality stays almost in a certain range with the increasing number of DRP slots per station. As we increase the number of video streams we observe after a certain number of DRP reserved slots per station, soft DRP performance gets degraded. With soft DRP, even more than 14 video streams can be supported with a small number of DRP slots per station. Hard DRP performance is even worse than the performance of PCA only case. With the PCA only case we find at most 12 video streams can sustain in the network with the satisfactory QoS requirement. Whereas the performance of hard DRP is the worst. It barely can support 12 video streams in the network.

From all these finding, researchers can make decision in which cases which mechanism should be adopted to get the optimal performance and also can tune the parameters, i.e. the number of video streams and the number of DRP reserved slots per station.

We also have shown the affected PCA performance when we modify the TXOP parameter for the high priority traffic. With the bigger TXOP, the high priority traffic gets performance improvement, however with the cost of the performance of

the low priority traffic.

## Chapter 7

# Conclusions and Future Work

High-quality video streaming is a very important and challenging problem in a household environment. Traditional wireless technologies, such as IEEE 802.11 and IEEE 802.15 families in some cases are not able to support high quality video streaming due to low data rate. Achievable data rate becomes even lower due to the high attenuation and interference in a household environment. Recently WiMedia Alliance working group has launched a new wireless technology, Ultra Wide Band, which supports very high data rate in short range. Its MAC layer has a special protocol, Distributed Reservation Protocol which allows any particular station to hold the channel exclusively. In order to investigate these features of UWB we have developed a small testbed with commercially available UWB products. From the measurement results we have found two important tradeoffs. First one is between TxRate and MAC layer transmission retry limit. Achievable throughput becomes higher due to increased TxRate, however higher retry limit sometimes reduces the achievable throughput. Second and the more interesting tradeoff we have got is the reservation pattern of DRP slots in the time cycle which is called superframe according to the WiMedia UWB standard. Clustered reserved slots result in higher throughput,

whereas scattered reservation reduces access delay or service delay to serve packets, but it suffers from a lower achievable throughput. These interesting findings help researchers to tune these parameters to have very high quality video streaming even for quad-HDTV H.264 encoded video streams. In this work I have modified D-ITG traffic generator [36] to obtain the accurate packet transmission delay by sending the ACK packet over the Ethernet.

To get the generalized view of UWB MAC we have brought the analysis and simulation approach in this research. Due to the limitation of commercially available products we could not experiment the performance of PCA protocol of UWB MAC. We have developed a model of UWB PCA protocol following the existing framework, renewal reward theorem considering without any DRP slot and with DRP slots interleaved with PCA slots. To validate this model we have developed the UWB MAC layer module in *NS-2* and also modified IEEE 802.11 physical layer to MBOA physical layer. Analysis results have been verified with the simulation results assuming traffic arrival pattern follows Poisson distribution. Taking this result as a base line we have investigated the H.264 encoded video streaming performance over UWB wireless networks. We have incorporated some distinct features of UWB MAC: soft DRP, hard DRP and TXOP. We found that the performance of video streaming is the best when we have some soft DRP co-existing with PCA time slots.

Other contributions of the thesis research are summarized as follows:

- We have built a multimedia over UWB wireless network testbed, and have established a guideline to tune some parameters to get the optimal video streaming performance. To obtain the transmission delay of a single packet we have modified the source code of D-ITG traffic generator.
- We have developed a UWB MAC layer simulation module with some special features such as soft DRP, hard DRP and TXOP. We also have developed a



dummy UWB physical layer.

- We have developed a set of programs to integrate *NS-2* and *EvalVid*.
- We have developed a model of UWB PCA protocol considering some hard DRPs interleaved with PCA time slots.

Our current research work has led us to some issues that need to be further explored. We list some of them as follows.

- **Block Acknowledgement:** Another feature of UWB MAC layer is Block Acknowledgement. To modify the analysis and simulation capturing Block Acknowledgement is the future direction of our research. We believe the maximum capacity of UWB wireless networks in terms of the number of video streams supported will be improved with this new feature.
- **Non-ideal Channel Condition:** In our study of this thesis, ideal channel condition is one of the assumptions. We set propagation delay to zero. However to capture the practical scenarios of UWB wireless networks we can use some propagation models to emulate a practical wireless channel. The future work is to study the video streaming performance in non-ideal wireless scenarios.
- **Heterogeneous traffic:** In our both simulation and analysis, we assumed each station holds one priority traffic. However according to the standard, multi-priority traffic can be incorporated in one station. Provisioning heterogeneous traffic per station is another piece of our future work.

# Bibliography

- [1] ECMA-368: High Rate Ultra Wideband PHY and MAC Standard, 2008.
- [2] X. Ling, K. Liu, Y. Cheng, X. Shen, and J. Mark, “A novel performance model for distributed prioritized MAC protocols,” in *Proc. IEEE GLOBECOM'07*, Nov 2007.
- [3] D. Li and J. Pan, “Performance analysis and evaluation of H.264 video streaming over multi-hop wireless networks,” in *Proc. IEEE GLOBECOM'08*, 2008, pp. 423–429.
- [4] G. Bianchi, “Performance analysis of the IEEE 802.11 distributed coordination function,” *IEEE Journal on Selected Areas in Communications (JSAC)*, vol. 18, no 3, pp. 535–547, March 2000.
- [5] E. Ziouva and T. Antonakopoulos, “CSMA/CA performance under high traffic conditions: Throughput and delay analysis,” *Computer Communications*, vol. 25, no. 3, pp. 313–321, Feb 2002.
- [6] Y. Wu, K. Long, S. Cheng, and J. Ma, “Performance of reliable transport protocol over IEEE 802.11 wireless LANs: Analysis and enhancement,” in *Proc. IEEE INFOCOM'02*, August 2002, pp. 599–607.

- [7] Y. Xiao and J. Rosdahl, "Throughput and delay limits of IEEE 802.11," *IEEE Communication Letters*, vol. 6, no. 8, pp. 355–357, Aug 2002.
- [8] K. Medepalli and F. Tobagi, "Throughput analysis of IEEE 802.11 Wireless LANs using an average cycle time approach," in *Proc. IEEE GLOBECOM'05*, May 2005, pp. 3007–3011.
- [9] X. Wang and J. Mellor, "Performance modeling of IEEE 802.11 DCF using equilibrium point analysis," in *Proc. IEEE AINA'06*, 2006.
- [10] J. Robinson and T. Randhawa, "Saturation throughput analysis of IEEE 802.11e enhanced distributed coordination function," *IEEE JSAC*, vol. 22, no. 5, pp. 917–928, June 2004.
- [11] Z. Kong, D. Tsang, B. Bensaou and D. Gao, "Performance analysis of IEEE 802.11e contention-based channel access," *IEEE JSAC*, vol. 22, no. 10, pp. 2095–2106, Dec 2004.
- [12] Y. Xiao, "Performance analysis of priority schemes for IEEE 802.11 and IEEE 802.11e wireless LANs," *IEEE Trans on Wireless Communications*, vol. 4, no. 4, pp. 1506–1515, July 2005.
- [13] P. Engelstad and O. Osterbo, "Non-saturation and saturation analysis of IEEE 802.11e EDCA with starvation prediction," in *Proc. ACM MSWiM'05*, Feb 2005, pp. 224–233.
- [14] M. Wong, F. Chin and Y. Chew, "Performance analysis of saturated throughput of PCA in the presence of hard DRPs in Wimedia MAC," in *Proc. ACM WCNC'07*, 2007, pp. 423–429.
- [15] R. Ruby, Y. Liu and J. Pan, "Evaluating video streaming over UWB wireless networks," in *Proc. ACM WMUNEP'08*, pp. 1–8, Oct 2008.

- [16] WiMedia, WiMedia Logical Link Control Protocol.  
available from <http://www.wimedia.org>
- [17] TKN EDCA Model for NS-2, 2006.  
available from <http://www.tkn.tu-berlin.de>
- [18] K. Kerpez, D. Waring, G. Lapiotis, J. Lyles, and R. Vaidyanathan, "IPTV service assurance," *Communications Magazine, IEEE*, vol. 44, no. 9, pp. 166–172, 2006.
- [19] T. Zahariadis, K. Pramataris, and N. Zervos, "A comparison of competing broadband in-home technologies," *Electronics & Communication Engineering Journal*, vol. 14, no. 4, pp. 133–142, 2002.
- [20] IEEE 802.11 Working Group, *IEEE Std. 802.11-1999, Part 11: Wireless LAN Medium Access Control (MAC) and Physical Layer (PHY) specifications*, IEEE Std., 1999.
- [21] IEEE 802.11 Working Group, *IEEE Std. 802.11e-2005, Amendment 8: Media Access Control (MAC) Quality of Service Enhancements*, IEEE Std., 2005.
- [22] J. Klaue, B. Rathke, and A. Wolisz, "Evalvid – a framework for video transmission and quality evaluation." [Online]. Available:  
<http://www.tkn.tu-berlin.de/research/evalvid/>
- [23] A. Netravali and B. Haskell, *Digital Pictures: Representation, Compression, and Standards*. Plenum Pub Corp, 1995.
- [24] "TCPDUMP – dump traffic on a network." [Online]. Available:  
<http://www.tcpdump.org>
- [25] "NO Ad-Hoc Routing Agent (NOAH)." [Online]. Available:  
<http://icapeople.epfl.ch/widmer/uwb/ns-2/noah/>

- [26] D. Li and J. Pan, "Evaluating MPEG-4 AVC video streaming over IEEE 802.11 wireless distribution system," *IEEE WCNC 2008*, pp. 2147–2152, 2008.
- [27] Y. Ye, J. Pan, M. Lu, L. Cai, and D. Hoffman, "Evaluating 'no-new-wires' home networks," *IEEE LCN WNM 2008*, 2008.
- [28] J. Pavon, N. Shankar, V. Gaddam, K. Challapali, and C. Chou, "The MBOA-WiMedia specification for ultra wideband distributed networks," *IEEE Communications Magazine*, 44(6):128–134, 2006.
- [29] W. Cui, P. Ranta, T. Brown, and C. Reed, "Wireless video streaming over UWB," *IEEE ICUWB 2007*, pp. 933–936.
- [30] C. Duan, G. Pekheryev, J. Fang, Y. Nakache, J. Zhang, "Transmitting multiple HD video streams over UWB links," *IEEE CCNC 2006*, pp. 691–695, 2006.
- [31] G. Hiertz, Y. Zang, J. Habetha, and H. Sirin, "IEEE 802.15.3a wireless personal area networks — the MBOA approach," *Proc. 11th Europe Wireless Conference*, pp. 204–210, 2005.
- [32] Y. Zang, G. Hiertz, J. Habetha, B. Otal, H. Sirin, and H. Reumerman, "Towards high speed wireless personal area network — efficiency analysis of MBOA MAC," *In Proc of Int'l Workshop on Wireless Ad-Hoc Networks 2005 (IWWAN 2005)*, pp. 10–20, 2005.
- [33] H. Wu, Y. Xia, and Q. Zhang, "Delay analysis of DRP in MBOA UWB MAC," *IEEE ICC 2006*, pp. 229–233, 2006.
- [34] K. Liu, X. Ling, X. Shen, and J. Mark, "Performance analysis of prioritized MAC in UWB-WPAN with bursty multimedia traffic," *IEEE Trans on Vehicular Technology*, vol. 57, no. 4, pp. 2462–2473, 2008.

- [35] Tzero: ZeroWire EVK, <http://www.tzerotech.com/products/zerowire-evk/>
- [36] D-ITG: Distributed Internet Traffic Generator, <http://www.grid.unina.it/software/ITG/>
- [37] IEEE 802.15TG3c: WPAN, <http://ieee802.org/15/pub/TG3c.html>
- [38] D.-J. Deng and R.-S. Chang, “A priority scheme for IEEE 802.11 DCF access method,” *IEICE Trans. Commun.*, vol. E82-B, no. 1, p. 96–102, Jan. 1999.
- [39] M. B. A. Veres, A. T. Campbell and L.-H. Sun, “Supporting differentiation in wireless packet networks using distributed control,” *IEEE J. Sel. Areas Commun.*, vol. 19, no. 10, p. 2081–2093, Oct. 2001.
- [40] I. Aad and C. Castelluccia, “Differentiation mechanisms for IEEE 802.11,” in *IEEE Information Communications (INFOCOM)*, 2001, p. 209–218.
- [41] X. Pallot and L. E. Miller, “Implementing message priority policies over an 802.11 based mobile ad hoc network,” in *IEEE Military Communications Conf. (MILCOM)*, 2001, p. 860–864.
- [42] A. Andreadis and R. Zambon, “QoS enhancement for multimedia traffics with dynamic txoplimit in IEEE 802.11e,” in *Q2SWinet07*, 2007, pp. 16–22.
- [43] H. S. J. Chul Geun Park and D. H. Han, “Queueing analysis of IEEE 802.11 mac protocol in wireless LAN,” in *ICNICONSMCL06*, 2006, pp. 1–6.
- [44] S. Shah-Heydari and T. Le-Ngoc, “MMPP models for multimedia traffic,” *Telecommunication Systems 15*, vol. 15, p. 273–293, Feb. 2000.
- [45] S. L. SCOTT and P. SMYTH, “The Markov modulated Poisson process and Markov poisson cascade with applications to web traffic modeling,” *BAYESIAN STATISTICS*, vol. 7, p. 001010, Feb. 2003.

- [46] F. Hartanto and H. R. Sirisena, "Cumulative inter-arrival jitter concept and its applications," in *ICNICONSMCL06*, 2006, pp. 1–6.
- [47] L. Xiong and G. Mao, "Saturated throughput analysis of IEEE 802.11e using two-dimensional markov chain model," in *QShine06*, 2006, pp. 1–10.
- [48] M. Hofri and Z. Rosberg, "Packet delay under the golden ratio weighted TDMA policy in a multiple-access channel," *IEEE Trans. Inform. Theory*, vol. 33, no. 3, p. 341–349, 1987.
- [49] I. Rubin and Z. Zhang, "Message delay and queue-size analysis for circuitswitched tdma systems," *IEEE Trans. Commun.*, vol. 39, no. 6, p. 905–914, 1991.
- [50] M. K. Khan and H. Peyravi, "Delay and jitter analysis of generalized demand-assignment multiple access (DAMA) protocols with general traffic," in *HICSS05*, 2005, pp. 1–10.
- [51] X. S. K.-H. Liu, H. Rutagemwa and J. W. Mark, "Efficiency and goodput analysis of Dly-Ack in IEEE 802.15.3," *IEEE Trans. Veh. Technol.*, vol. 56, no. 6, p. 3888–3898, 2007.
- [52] R. Y. H. Chen, Z. Guo, X. Shen, and Y. Li, "Performance analysis of delayed acknowledgment scheme in UWB-based high-rate WPAN," *IEEE Trans. Veh. Technol.*, vol. 55, no. 2, p. 606–621, 2006.
- [53] X. S. Y. Xiao and H. Jiang, "Optimal ACK mechanisms of the IEEE 802.15.3 MAC for ultra-wideband systems," *IEEE J. Select. Areas Commun.*, vol. 24, no. 4, p. 836–842, 2006.
- [54] A. Fukuda and S. Tasaka, "The equilibrium point analysis - a unified analytic tool for packet broadcast networks," in *Proc. IEEE Globecom83*, 1983, p. 1–33.

- [55] D.-M. C. Y. Gao and J. C. S. Lui, “Determining the end-to-end throughput capacity in multi-hop networks: methodology and applications,” in *Proc. ACM SIGMETRICS06*, 2006, pp. 39–50.
- [56] L. Kleinrock and F. A. Tobagi, “Packet switching in radio channels: Part I Carrier sense multiple-access modes and their throughput-delay characteristics,” *IEEE Trans. Commun.*, vol. 23, no. 12, p. 1400–1416, 1975.
- [57] J. Zheng and M. J. Lee, “Will IEEE 802.15.4 make ubiquitous networking a reality? - a discussion on a potential low power, low bit rate standard,” *IEEE Commun. Mag.*, vol. 42, no. 6, p. 140–146, 2004.
- [58] D. Bertsekas and R. Gallager, ”Data Networks,” Prentice Hall, 2nd edition, 1992.
- [59] *IEEE. Wireless Medium Access Control (MAC) and Physical Layer (PHY) specifications for low-rate wireless personal area networks (LR-WPANs) (IEEE 802.15.4)*, 2003.